# Innovative Solutions for Low Power Photovoltaic Water Pumping Systems - Development of a DC-DC Step-up Converter

**Alice Nogueira Fey**

Dissertation presented to the School of Technology and Management - Polytechnic Institute of Bragança - to the fulfillment of the requirements for the Master of Science Degree - Renewable Energy and Energetic Efficiency - in the scope of Double Degree with Federal University of Technology - Paraná

Supervised by:

Professor Ph.D. Américo Vicente Teixeira Leite

Professor Ph.D. Eduardo Félix Ribeiro Romaneli

This work does not include the appointments and suggestions of the Jury

Bragança

2020

# Soluções Inovadoras para Sistemas Fotovoltaicos de Bombeamento de Água de Baixa Potência - Desenvolvimento de um Conversor CC-CC Elevador

**Alice Nogueira Fey**

Dissertação apresentada a Escola de Tecnologia e Gestão - Instituto Politécnico de Bragança - para atender aos requerimentos do curso de Mestrado - Energias Renováveis e Eficiência Energética - no escopo de dupla diplomação com a Universidade Tecnológica Federal do Paraná.

Supervisado por:

Professor Dr. Américo Vicente Teixeira Leite

Professor Dr. Eduardo Félix Ribeiro Romaneli

Este trabalho não inclui os apontamentos feitos pelo júri.

Bragança

2020

FÜR TÄNZER

Glattes Eis

Ein Paradeis

Für Den, der gut zu tanzen weiss.

(NIETZSCHE, Friedrich W.)

# Acknowledgments

To my parents and my sister, who supported me in the graduation journey and made possible this double diploma opportunity. Without their support, my life would not be as great as it is.

To my beloved friends Aron Ludovico, Bruna Odilia, Bruna Paludo, Bruno Appel, Carlos Henrique, Fernando Helfenstein, Fernando Pikler, José Baggio, Julia Zibetti, Olívia Nichele, Sabrina Boaretto, Sarah Gruetzmacher and Victor Avila, who were always by my side and helped me through the tough times, even when I had lost faith in myself.

To the women that are my daily inspiration, my godmother Idanir Bonato and my grandmother Judite Fey, who helped raising me and taught me how to stay strong and be kind to others.

To my professors Eduardo Romaneli, who encouraged me from the beginning and taught me a lot, and Vicente Leite, who accepted to be my supervisor, helped me and made me change my point of view on several things.

To the teachers and friends of the LSE (Laboratório de Sistemas Eletromecatrônicos), who always helped me when needed.

To the company VALLED, for supporting the development of the present work and providing the equipment needed during experimental validations.

At last, but not least, to the Federal University of Technology - Paraná (UTFPR), Campus Curitiba and the Polytechnic Institute of Bragança (IPB) for the exchange opportunity and for all the effort held to make this research possible.

# Abstract

It is known that the use of Photovoltaic Water Pumping Systems (PVWPS) is a solution to supply water to populations living in arid and remote regions. But there are still problems regarding costs and market availability of PVWPS. These systems are usually sold as closed kits and with solar energy dedicated equipment. This situation makes it difficult to replace damaged equipment for other that would be available on the market. Also, solar dedicated equipment are more expensive than the general-purpose ones. Another issue is the oversizing of the PV panel in terms of power, when installing low power PVWPS that employ conventional AC motor-pumps. The oversizing occurs in order to achieve the voltage requirements of these water pumps.

With the aim of solving the problems mentioned above, this work proposes four innovative solutions for low power PVWPS. The proposed solutions are for installations up to 750W (1HP); employ a maximum of 4 photovoltaic modules; are composed of standard frequency converters and AC motor-pumps. Also, a simple and cost-effective DC-DC voltage step-up converter was conceived to be a part of the suggested PVWPS. It was designed and tested a 750W DC-DC step-up converter with a static gain of 3.44.

One of the proposed solutions for low power PVWPS employing the designed DC-DC step-up converter was tested in a laboratory environment and successfully validated. The system was tested under distinct weather conditions and showed promising results. It was verified that is possible to conceive a PVWPS based on standard frequency converters and other conventional components.

The present work was made in cooperation with the company VALLED. The goal was to work together with the company in order to develop a modular, reliable, robust and cost effective solution.

**Keywords:** Photovoltaic Water Pumping, Frequency Converter, Switched-Capacitor Double Boost Converter, AC Motor-pump, Photovoltaic Energy**.**

# Resumo

Sabe-se que o uso de sistemas fotovoltaicos de bombeamento de água (SFVBA) vieram como uma solução para fornecer água a populações que vivem em regiões áridas e remotas. No entanto, ainda existem problemas em relação aos custos e disponibilidade no mercado dos SFVBA. Esses sistemas geralmente são vendidos como conjuntos fechados e com equipamentos dedicados à energia solar. Essa situação dificulta a substituição de equipamentos danificados por outros que estariam disponíveis no mercado. Além disso, os equipamentos dedicados a uso com energia solar são mais caros que os de uso geral. Outra questão é o superdimensionamento do painel fotovoltaico em termos de potência, ao instalar SFVBA de baixa potência que empregam motobombas CA convencionais. O sobredimensionamento ocorre para que se atinjam os requisitos de tensão dessas bombas de água.

Para solucionar os problemas mencionados acima, este trabalho propõe quatro soluções inovadoras para SFVBA de baixa potência. As soluções propostas são para instalações de até 750W (1HP); empregam no máximo 4 módulos fotovoltaicos; são compostas por conversores de frequência padrão e motobombas CA. Além disso, para compor os SFVBA sugeridos, um conversor CC-CC elevador de tensão com estrutura simples e econômica foi concebido. Foi projetado e testado um conversor CC-CC elevador de tensão de 750W com um ganho estático de 3,44.

Uma das soluções propostas para SFVBA de baixa potência empregando o conversor CC-CC projetado foi testada em um ambiente de laboratório e validada com sucesso. O sistema foi testado sob condições climáticas distintas e mostrou resultados promissores. Verificou-se que é possível conceber um PVWPS baseado em conversores de frequência de uso geral e outros componentes convencionais.

O presente trabalho foi realizado em cooperação com a empresa VALLED. O objetivo era trabalhar em conjunto com a empresa para desenvolver uma solução modular, confiável, robusta e econômica.

**Palavras-chave:** Bombeamento Fotovoltaico, Inversor de Frequência, Conversor Duplo-Boost a Capacitor Chaveado, Motobomba CA, Energia Solar Fotovoltaica.

# Contents

# List of Tables

# List of Figures

# Acronyms

| | |
|---|---|
| AC | Alternating Current |
| CCM | Continuous Current Mode |
| DC | Direct Current |
| ESTiG | Escola Superior de Tecnologia e Gestão |
| HW | Hardware |
| IM | Induction Motor(s) |
| IPB | Polytechnic Institute of Bragança |
| $I_{MPP}$ | Maximum Power Point Current |
| $I_o$ | Output Current |
| Ki | Integral Time |
| Kp | Proportional Gain |
| LSE | Laboratory of Electromechatronics Systems |
| MPP | Maximum Power Point |
| MPPT | Maximum Power Point Tracking |
| PI | Proportional Integral |
| PID | Proportional Integral Derivative |
| PMSM | Permanent Magnet Synchronous Motors |
| PWM | Pulse Width Modulation |
| PV | Photovoltaic |
| PVWPS | Photovoltaic Water Pumping System(s) |
| RMS | Root Mean Square |
| SCDB | Switched-Capacitor Double Boost |
| SFC | Standard Frequency Converter |
| $V_i$ | Input Voltage |
| $V_{MPP}$ | Maximum Power Point Voltage |
| $V_{oc}$ | Open-Circuit Voltage |
| $V_o$ | Output Voltage |

# 1. Introduction

## 1.1. Context

As the environmental concerns are growing, the migration to cleaner and greener energy sources is becoming a natural movement. Among all of the renewable energy sources, solar energy is the most economical, efficient and easily traceable [1]. In this scenario, the employment of solar Photovoltaic (PV) energy increases each year. PV systems are present from small power application, such as houses and public lighting, to large power systems, like industries and remote areas power plants. PV arrays are also employed in low and medium water pumping facilities, for both irrigation purposes and water supply to communities [1].

In arid regions, where there is abundant solar irradiance and the sun is the greatest energy source, PV water pumping came as strategic solution to supply drinkable water to marginal populations. A 2017 report published by The Guardian, based on a World Health Organization data, exposed that "Since 1990, 2.6 billion people have gained access to an 'improved' drinking water source, one that is designed to protect against contamination. But in 2015, 663 million people – one in 10 – still drank water from unprotected sources" [2]. The **Figure 1** shows an infographic representing the percentage of population using unimproved drinking water source around the world.

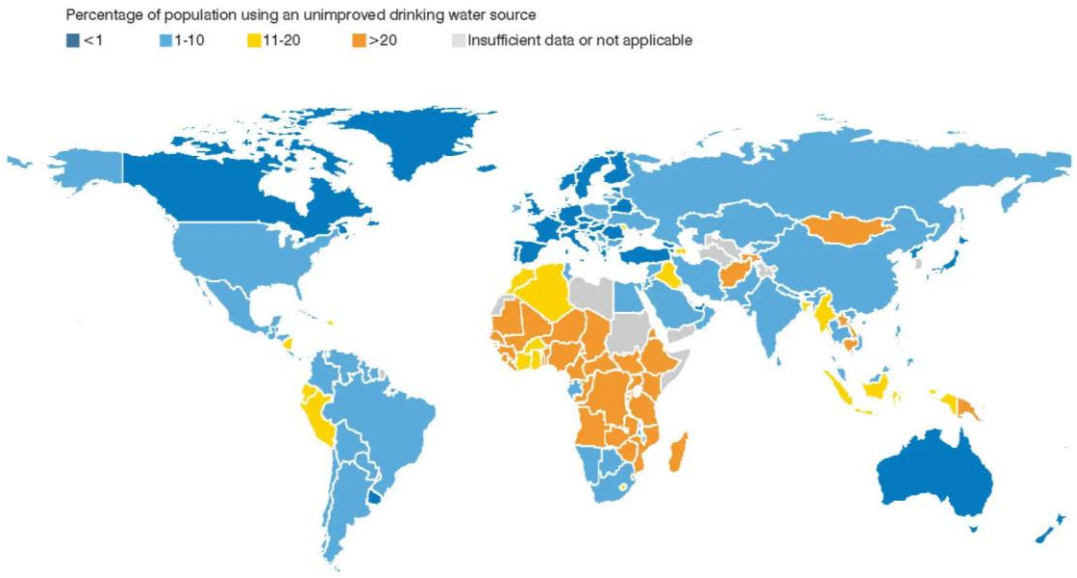


**Figure 1:** World map of people with access to unimproved drinking water sources [2].

When considering the installation of PV water pumping systems (PVWPS) in remote and poor regions, the cost of the system and the maintenance requirements are very important aspects. For small-scale facilities, PVWPS require no batteries, thus the water tank acts as the storage solution. This avoids most technical losses and the high costs of periodic battery replacement. Compared to diesel generators, PV-driven pumps have minimal maintenance requirements and are more cost-effective [3]. The **Figure 2** shows the running costs of the water supply pumping technologies.

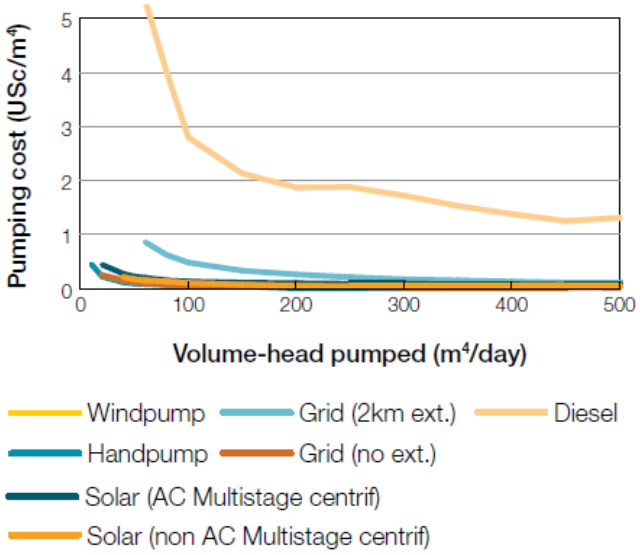


**Figure 2:** Running costs of water supply pumping technologies [3].

One of the countries that stands on the situation where more than 20% of its population does not have access to reliable source of drinkable water is Angola – Africa (as seen previously in **Figure 1**). The Angolan government developed a project called "Água para Todos" ("Water for All") [4]. It started in 2007 with goals to promote access to drinkable water for marginalized populations, who live in a precarious water supply scenario. In the scope of the project, published by the Ministry of Energy and Waters of Angola, it was stated that the administrations should privilege the execution of simple and easy to operate systems, emphasizing the use of wells with electric pumps powered by solar PV panels. In the context of the budget estimate, the reference document also stated that priority should be given to the execution of solutions based on solar PV pumps [4].

A report published by "Jornal de Angola" in March 2020 showed the current status of the "Água para Todos" program. The interviewed State Secretary for Water

commented that the government should at least double the investments in water supply. It was said that, for example, Luanda (by this date) only has, in terms of production capacity, something like 40 to 50 percent of what it needs to have a minimally comfortable situation regarding drinkable water supply. The main problem highlighted was the lack of investment resources [5].

In this context, the company VALLED (Bragança-based enterprise) is one of the suppliers of solar PV pumping solutions to the Angolan government. Due to the recurring demand for low power PVWPS that are robust and low cost, VALLED (http://www.valled.pt/), together with IPB, seeks innovative solutions that suit the installation requirements.

### 1.2. Problem Formulation and Motivation

When looking for solar water pumping solutions, the main problem seen is that PVWPS are generally sold as a closed kit, making it difficult and expensive to replace failed equipment for others that would be available on the market [6]. Also, solar energy dedicated equipment are usually more expensive than the general-purpose ones.

Some meetings held with representatives of VALLED showed another recurring problem, mostly faced when designing low power PVWPS that employ conventional AC motor-pumps. The problem is the oversizing of the PV panel in terms of DC power. The oversizing occurs in order to achieve the voltage requirements of the connected equipment that will run the water pump. For example, to run a 750W/230$V_{ac}$ water pump is needed, in terms of power, a maximum of 4 PV modules (275W/31.5$V_{MPP}$ conventional ones), but in terms of voltage it is needed at least 8 PV modules.

All these exposed problems affect the financial costs of PVWPS projects, thus the present work intend to solve them. When talking about market competitivity and solutions for customers with limited resources and purchasing power, the financial matter is the main issue.

Previous works regarding low power PVWPS solutions already showed that Standard Frequency Converters (SFCs) and other general-purpose equipment used in industrial applications can be employed in systems powered by PV generators [6] - [10]. Thus, the integration of SFCs to PVWPS can solve the problems of costs regarding the use of solar energy dedicated equipment. Also, general-purpose equipment have greater availability on the market, which facilitates the replacement in cases of damage. It means that users become independent, not relying on just one supplier.

In order to solve the oversizing challenge of the PV panel in low power PVWPS, the solution is to add a voltage boosting stage between the PV modules and the SFC. The voltage boosting can be obtained by using a DC-DC step-up converter. This converter would “replace” the additional PV modules, which are needed to achieve the requested DC voltage for running the AC motor-pump.

The present work intends to design a solution as “market ready” as it can be, that can turn into a product. For a company to have a product of its own, it means independence and market opening. The greatest motivation is to reach the current PVWPS market in a competitive way. Thus, the importance of developing a simple module that can integrate a PV panel and an SFC in order to compose a cost effective low power PVWPS.

### 1.3. Goals

The main goal of the present work is to develop a competitive low power PVWPS solution (1kW maximum), based on an SFC and a DC-DC step-up converter, employing only conventional components (from a company perspective). The secondary goals are summarized as follows:

- Research the and propose frequency converters available on market that would be suitable for operating with PV energy as its input and running a water pump up to 1kW.
- Design and test a step-up DC-DC converter suitable for boosting the PV voltage levels according to the requirements of SFCs inputs.
- Ensure that the oversizing challenge, regarding the PV power, is addressed.
- Compose a PVWPS without the use of battery and electrical energy storage components.
- Design a control responsible to act as similar as the MPPT algorithms employed on standard Solar Inverters, that can also protect the system in case of a sudden shutdown.
- Suggest few solutions for low power PVWPS describing the possible layout and equipment needed.
- Test at least one low power PVWPS solution based on the DC-DC step-up converter developed and provide steady results.

## 1.4. Document Structure

This dissertation is divided into six sections. The contents are as follows:

1. **Introduction:** this section describes the global and local context of the work, as well as the problem intended to be solved, the motivation and objectives.
2. **PV Water Pumping Systems:** presents the state of the art of PVWPS application that is relevant regarding the context. It describes the main components, the previous solutions and the current market situation.
3. **Proposed Solution for Low Power PVWPS:** presents the PVWPS solutions and the related equipment. It is also described the choice and theoretical design of the DC-DC step-up converter.
4. **Hardware Validation:** describes how the hardware validation was held; the components used; and the tests conditions.
5. **Results and Discussion:** exposes the tests results and analysis, as well as the challenges and the difficulties encountered along the way.
6. **Conclusions and Future Work:** the last section summarizes the whole work and proposes future works activities.

# 2. PV Water Pumping Systems

## 2.1. Overview

The latest developed Photovoltaic Water Pumping Systems are basically composed of a solar PV generator, a frequency converter (with or without a step-up voltage stage), a filter and a pump set. The frequency converter is responsible for conditioning the DC energy generated by the PV panel into an AC controlled energy. There are PVWPS that employ batteries, at the DC-link of the frequency converter, to ensure better control of the energy and voltage levels [11]. **Figure 3** represents the main PVWPS components.

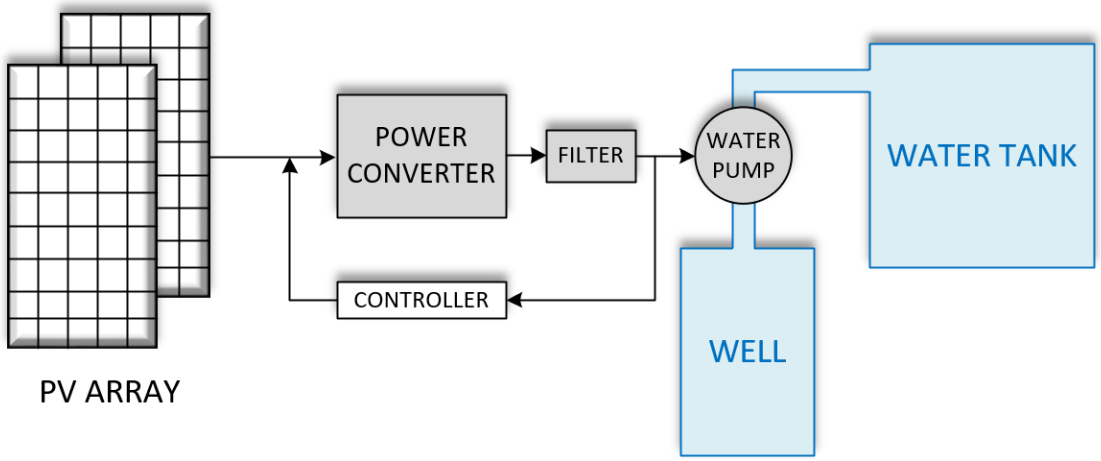


**Figure 3**: Main components of a PVWPS. Image adapted from [11].

There are several types of PVWPS, composed by different kind of equipment. The ones with pumps operated by DC motors and other operated by AC induction motors (IM). PVWPS also may contain batteries and be installed within the most varied power levels (with pumps from 0.5 to 5HP).

The issue about PVWPS without batteries and other electrical energy storage elements is that they are designed to pump water only during the day. This system functioning is totally dependent on the amount of sunlight hitting the PV panel. Also, the quantity of pumped water (power/speed of the pump) changes throughout the day, due to the sun irradiance, the angle at which it strikes the PV panel and possible shadings. PVWPS without batteries are sized to store extra water on sunny days, so that it is

available on cloudy days and at night. Water-storage capacity is essential in this kind of pumping systems [12].

### 2.1.1. Frequency Converters

A frequency converter is also known as “inverter”, “AC drive”, “adjustable-frequency drive”, “variable frequency controller”, “variable-speed driver”, etc. This equipment consists of a power electronics conversion structure, usually composed of three distinct parts: a rectifier bridge, a DC-link, and an inverter bridge. The frequency converter may or may not present an initial voltage boosting stage. There are some distinct types of frequency converters, but most drives are AC-AC ones, thus they convert AC input to a conditioned AC output [14].

**Figure 4** presents a diagram of a standard frequency converter. This is an equipment used in electro-mechanical drive systems to control an AC motor speed and torque, by varying the motor input frequency and voltage. SFCs are widely used and are a consolidated technology in the market, thus have competitive prices. They are employed in many industrial applications, to run equipment like fans, pumps, blowers, cranes, elevators, etc.

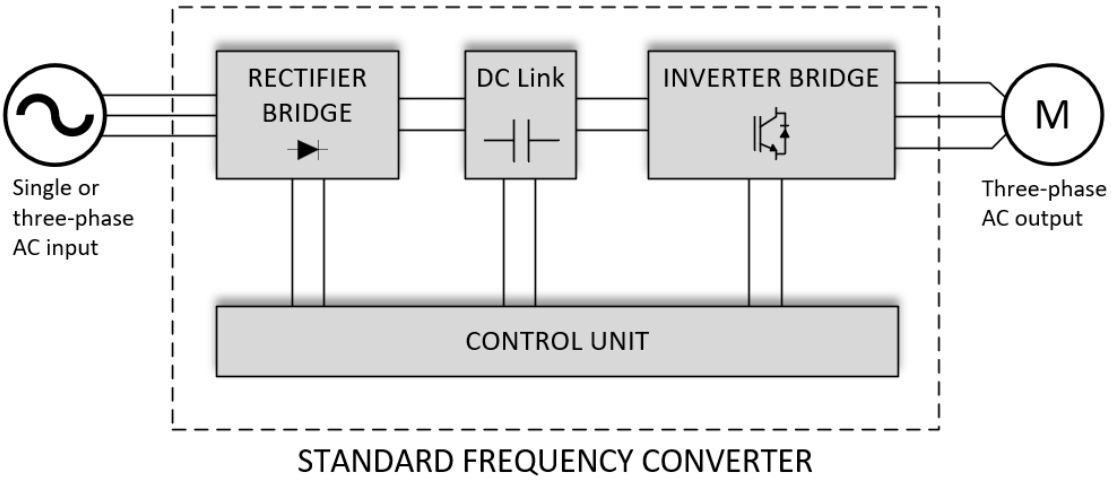


**Figure 4:** Standard Frequency Converter diagram. Image adapted from [7].

Single-phase input SFCs models are available in 110-127$V_{ac}$ and 200-240$V_{ac}$. These models employ different circuits to synthesize the input voltage to their DC-link. Models that work with 110-127$V_{ac}$ have a voltage booster circuit at their input in order to provide the DC-link voltage required by the DC-AC stage. The models that operate with

200-240$V_{ac}$ input voltage are seen with a rectifier circuit at the first stage [14]. The three-phase input SFCs are usually seen within voltage ranges from 200-240$V_{ac}$ and 380-480$V_{ac}$.

Among the main SFCs manufacturers are ABB, WEG, Yaskawa, Allen Bradley, Siemens, Schneider, Leroy Somer and Control Techniques. The minority of the SFCs available on the market are single-phase input and output. The most commonly found SFCs are three-phase input/output, with voltage ratings of 200-240$V_{ac}$ and 380-480$V_{ac}$.

The SFCs were designed to operate with an AC input, but previous works already shown that they can operate with DC input from PV modules [6] - [10]. By analyzing the most common topology of SFCs (**Figure 4**), it can be concluded that the effect of a DC input in the SFC functioning is that the rectifier stage will not be needed, thus the input current will flow just by one arm of the rectifier bridge. Also, when checking technical manuals of frequency converters, it can be seen that some of them features the DC input possible ratings. As an example, it is shown in **Figure 5** part of the technical manual from the Yaskawa J1000 AC drives. These are general-purpose frequency converters for industrial applications. The highlighted part of the image shows the rated DC input voltage of the SFC.

| Item | | | | Specification | | | | | | |
|---|---|---|---|---|---|---|---|---|---|---|
| Three-Phase Drive Model | | | | 2A0001 | 2A0002 | 2A0004 | 2A0006 | 2A0010 | 2A0012 | 2A0020 |
| Single-Phase Drive Model <1> | | | | BA0001 | BA0002 | BA0003 | BA0006 | BA0010 | - | - |
| Maximum Motor Size Allowed (HP) <2> | | | ND Rating | 0.125 & 0.25 | 0.25 | 0.5 & 0.75 | 1.0 & 1.5 | 2.0 & 3.0 | 3.0 | 5.0 |
| | | | HD Rating | 0.125 | 0.25 | 0.5 | 0.75 & 1 | 2.0 | 3.0 | 5.0 |
| Input | Input Current (A) <3> | Three-Phase | ND Rating | 1.1 | 1.9 | 3.9 | 7.3 | 10.8 | 13.9 | 24.0 |
| | | | HD Rating | 0.7 | 1.5 | 2.9 | 5.8 | 7.5 | 11.0 | 18.9 |
| | | Single-Phase | ND Rating | 2.0 | 3.6 | 7.3 | 13.8 | 20.2 | - | – |
| | | | HD Rating | 1.4 | 2.8 | 5.5 | 11.0 | 14.1 | - | - |
| Output | Rated Output Capacity (kVA) <4> | | ND Rating | 0.5 | 0.7 | 1.3 | 2.3 | 3.7 | 4.6 | 7.5 |
| | | | HD Rating | 0.3 | 0.6 | 1.1 | 1.9 | 3.0 | 4.2 | 6.7 |
| | Output Current (A) | | ND Rating <5> | 1.2 | 1.9 | 3.5 (3.3) | 6.0 | 9.6 | 12.0 | 19.6 |
| | | | HD Rating | 0.8 <6> | 1.6 <6> | 3.0 <6> | 5.0 <6> | 8.0 <7> | 11.0 <7> | 17.5 <7> |
| | Overload Tolerance | | | ND Rating: 120% of rated output current for 1 minute<br>HD Rating: 150% of rated output current for 1 minute<br>(Derating may be required for applications that start and stop frequently) | | | | | | |
| | Carrier Frequency | | | 2 kHz (user-set, 2 to 15 kHz) | | | | | | |
| | Max Output Voltage (V) | | | Three-phase power: 200 to 240 V<br>Single-phase power: 200 to 240 V<br>(both proportional to input voltage) | | | | | | |
| | Max Output Frequency (Hz) | | | 400 Hz (user-adjustable) | | | | | | |
| Power Supply | Rated Voltage<br>Rated Frequency | | | Three-phase power: 200 to 240 V 50/60 Hz<br>Single-phase power: 200 to 240 V 50/60 Hz<br>DC power supply: 270 to 340 V <8> | | | | | | |
| | Allowable Voltage Fluctuation | | | -15 to 10% | | | | | | |
| | Allowable Frequency Fluctuation | | | ±5% | | | | | | |
| Harmonic Corrective Actions | | DC Link Choke | | Optional | | | | | | |

**Figure 5:** Yaskawa J1000 AC drives - Technical specification [15].

The effect of a DC input in the SFCs that contain an initial boosting stage (110-127$V_{ac}$ input / 200-240$V_{ac}$ output) has to be studied. The topology of each designated frequency converter has to be analyzed to conclude whether or not a DC input voltage would also be boosted.

For a suitable operation in a PVWPS, the SFC must contain an internal PI controller. The frequency converter has to operate in closed loop control, with the PV panel voltage as the control variable [14]. The function of the PI controller in an SFC is to adjust its operation parameters, so that the input voltage is equal to the set reference voltage. Thus, the PV array will operate at a constant voltage, regardless the changes of irradiance, of temperature and partial shadings [10].

### 2.1.2. Motor-pumps

Hydraulic motor-pumps are machines that convert mechanical energy from an electric motor into kinetic energy and pressure of the pumped fluid. In PVWPS, the centrifugal pump works at different speeds according to the available solar irradiance [14].

The motor-pumps used in PVWPS are seen employing DC and AC motors, these ones can be found either single or three-phase. The AC motors, mainly the induction motors (IM) have their own limitations. They present lower efficiency in comparison to DC brushless motors, as well as poor starting performance. The initial operation of an IM is complicated due to large stator resistance voltage drop and slip needed to produce desired torque [16]. In contrast, the DC motors (brushless permanent magnet ones) are much easier to operate with PV systems, however, they have big disadvantages of regular maintenance, lack of robustness and they are not as available on the market as the AC motors [16]. These disadvantages make DC motors not suitable for applications in isolated areas, where there is no specialized personnel for operating and maintaining these motors [17].

There are basically two types of hydraulic motor-pumps: positive displacement and centrifugal. They can either be submersible or surface pumps. The main difference from positive displacement to the centrifugal ones, resides on the fluid path inside the pump. In the first ones, the fluid at the system outlet has approximately the same direction as the inlet and is driven by pistons. In the last ones, the fluid is displaced by the rotor blades, which change its pression and direction [6]. **Figure 6** shows the difference between centrifugal and positive displacement pumps.

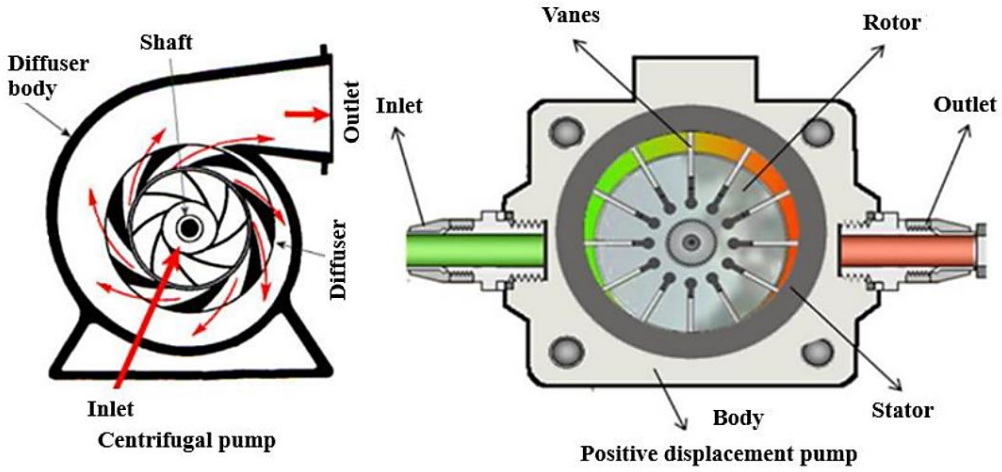


**Figure 6:** Centrifugal and positive displacement pumps [18].

Due to the high resistant torque exerted on the engine in ordinary positive displacement pumps, a greater starting power is needed from the engine. Thus, when considered a PV-fed system, it implies on a larger PV generator. Although, in the last years, the helical pumps (positive displacement type) has shown good functioning and with high efficiencies, being well suited for PVWPS [6], [19].

Among the main local and global manufacturers of motor-pumps can be mentioned, respectively, LORENTZ, Pentax and Ideal Delta, as well as Grundfos, Wilo and ETEC.

The water pump manufacturer LORENTZ has submersibles helical rotor-pumps, which are sold to be employed in PVWPS. It is disclosed on the manufacturer's website that the LORENTZ helical positive displacement pumps present high efficiency and ability to produce high pressure, consequently, the water pumping can start early in the day when the solar power is low and continuing to run late into the afternoon [20].

In the scope of the submersible centrifugal pumps used in PVWPS, can be cited the ones commercialized by the manufacturers LORENTZ and Ideal Delta. **Figure 7** presents LORENTZ and Ideal Delta submersible water pumps.

**(a)** **(b)** **(c)**

**Figure 7:** Submersible water pumps - **(a)** LORENTZ HR helical [20] **(b)** LORENTZ centrifugal [21] **(c)** Ideal Delta centrifugal [22]

In [14] it is presented that water pumps driven by PV energy, in almost all the working period, operate at frequencies below the nominal frequency. Thus, the recommendation is that, for a given manometric head (H), one should select a pump whose operating point on the H-Q curve at the nominal frequency is positioned to the right of its best efficiency line.

For example, to a given 60Hz water pump, which H-Q curve is shown in **Figure 8**, the ideal working head would be around 31mH2O. That is because when this PV-driven pump is operating in a frequency around 56Hz, at 31mH2O the best efficiency curve meets the H-Q curve. Then, this pump would be working at its maximum efficiency. When choosing an operating point whose efficiency its higher at frequencies below nominal, it is possible to increase the average daily yield of the PVWPS.

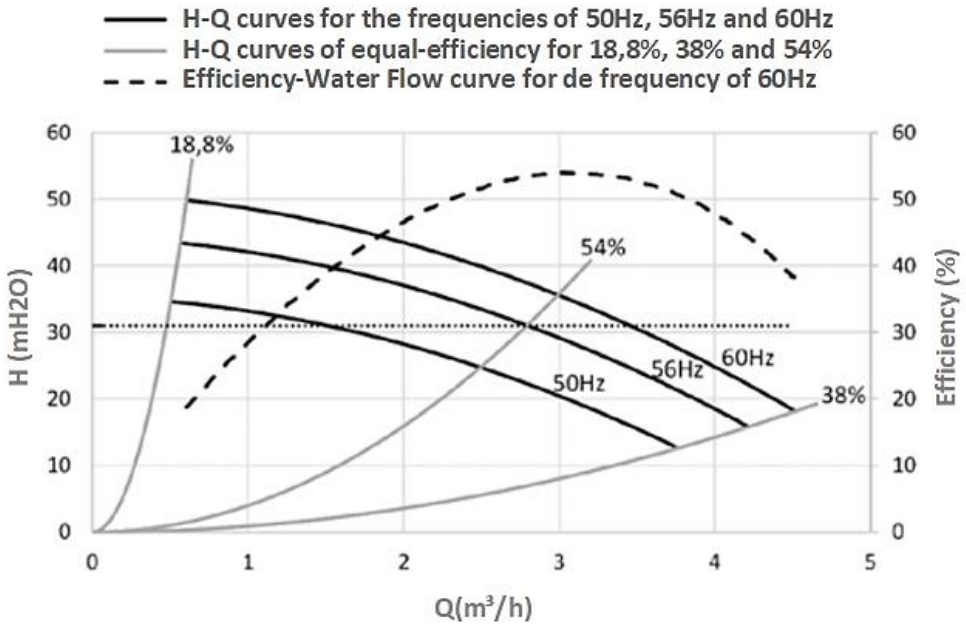


**Figure 8:** An example of a 60Hz water pump H-Q curve. Image adapted from [14].

## 2.2. Previous Works – A Review

It was carried out an extensive research on theses, dissertations and published articles related to PVWPS. Most of the solutions presented in literature are for three-phase IM-driven pumps, many of which proposes topologies of two-stage converters, with voltage boosting and a full bridge inverter. The minority of the solutions are for low power PVWPS employing equipment already available on the market.

In [19] and [23] is presented a complete and detailed review of the existing structures of PVWPS as well as the technologies involved. It is also presented the world situation regarding the employment of PVWPS and the promising technologies of converters, controllers and water pumps. **Figure 9** presents a summary of the PVWPS existing structures.

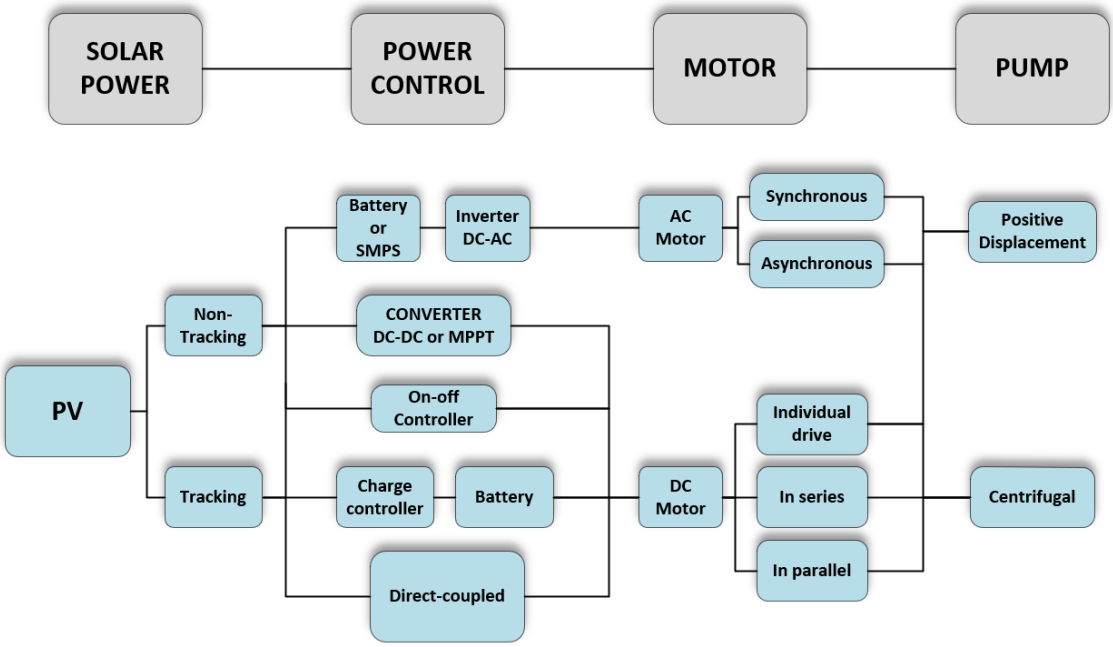


**Figure 9:** PVWPS structures outline. Image adapted from [23].

In [1], [16], [17], [24], [26], [27] and [28] are presented solutions for PVWPS based on two-stage converters. The suggested topologies for the converters involve a first DC-DC voltage boosting stage, connected with a DC-AC inverter. In the inverter stage it is mostly encountered the full-bridge topology and the employed water pumps are mostly driven by IM. **Figure 10** shows some of the solutions topologies proposed by the cited authors.

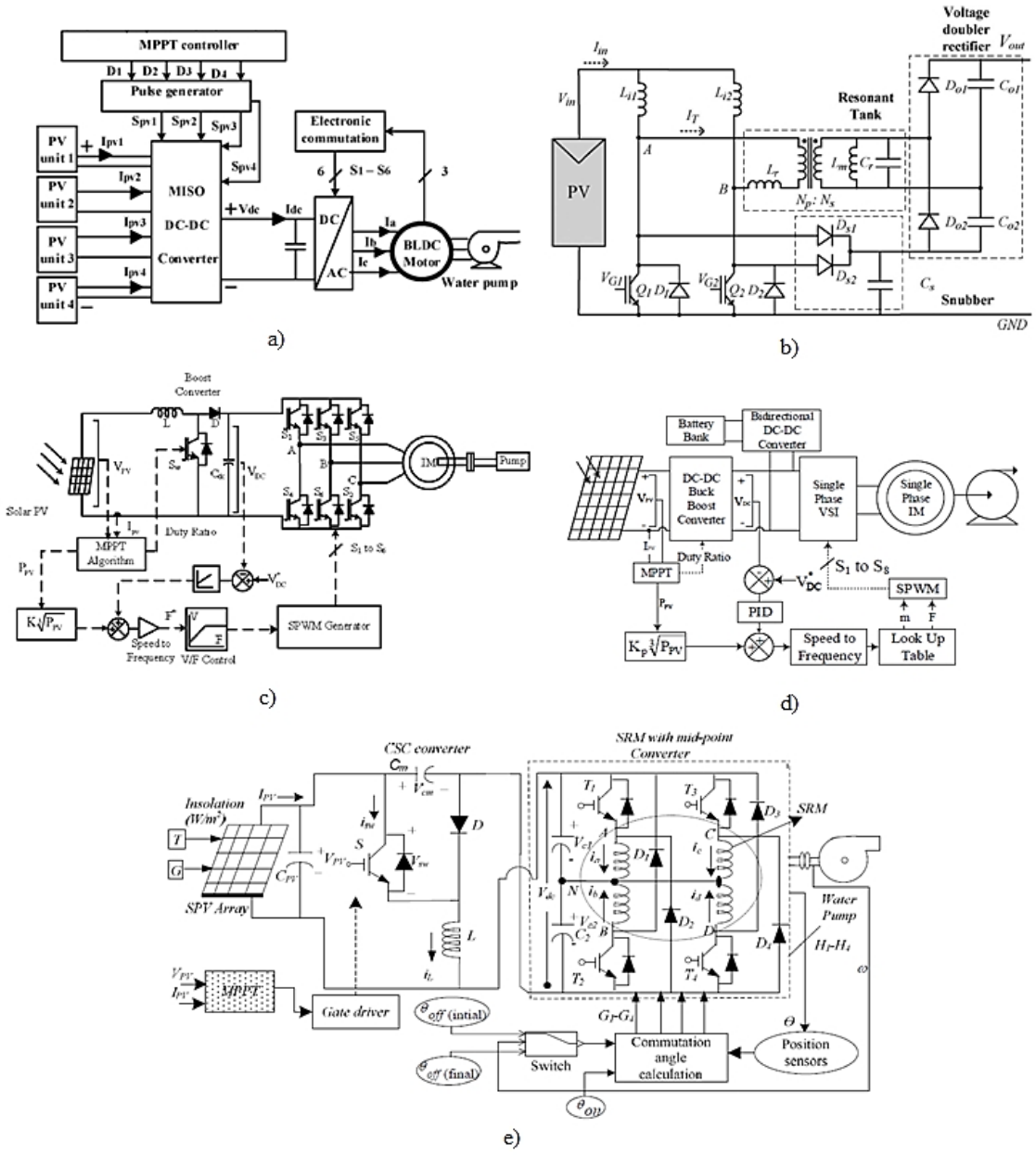


**Figure 10:** Topologies for PVWPS solutions. – (a) [24] (b) [17] (c) [28] (d) [1] (e) [16]

In [6] is presented a comparison between PVWPS composed by a combination of equipment exclusively built for PV application and general purpose ones. It was tested PVWPS with a PV inverter (1.5kW/85-140V); an SFC (2.2kW/220$V_{ac}$/3 phase); a conventional low cost water pump (0.56kW/220V); and a PV water pump (0.56kW/68V). It was verified that the performance of all the tested systems is completely related to the incident solar irradiance levels. It is also concluded that PVWPS with PV-dedicated inverters present a lower critical level of irradiance, pumping water earlier in the day and continuing later in the afternoon. This is due to the presence of MPPT in the PV inverters.

In [10], it was proposed and tested a solution for a 1.2kW PVWPS employing an SFC and a centrifugal pump driven by a $220V_{ac}$ three-phase IM. The **Figure 11** shows a diagram of the tested system. The results were presented in great detail. This type of PVWPS solution proved to be advantageous in comparison to systems with PV-dedicated inverters and pumps. The prices of SFCs are lower than the PV-dedicated equipment and a wider power range is available. This type of solution [10] provides an open window on the PVWPS market, being a great strategy for the manufacturers.

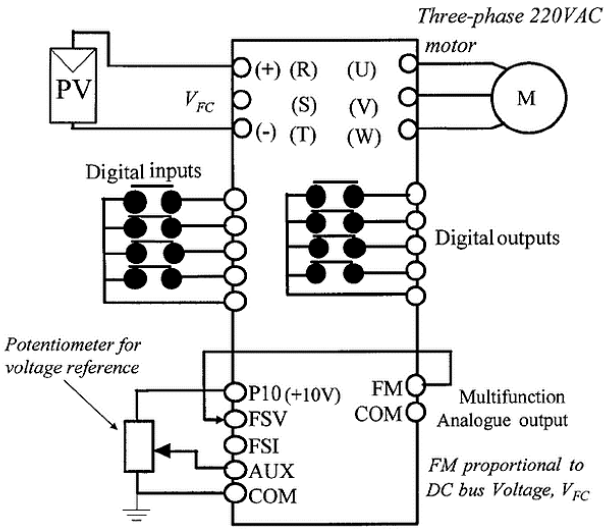


**Figure 11:** Solution for PVWPS presented in [10].

In [25] it is also proposed a PVWPS employing an SFC. The system tested was composed by a 2.5kW PV panel; an SFC connected to a digital control board with V/f control algorithm; and a 1.85kW centrifugal motor-pump. The new approach came by using an external control board to improve the SFC-based PVWPS performance. The results showed that employing SFCs with conventional scalar control results on frequent shutdowns of the PVWPS; on limitation of water pumping periods along the day; and on non-optimal IM efficiency. Another problem seen when using an SFC is the lack of protection in cases when the motor-pump is operating without load.

Previous works carried out at LSE (IPB) have already proposed solutions for PVWPS based on standard components. In [7], [8] two types of PVWPS based on SFCs were suggested. Systems with battery storage and charge controllers were tested, as well as a system with DC-DC Boost converter. In [9] different type of PVWPS composed by battery, charge controller and SFC were proposed and tested.

## 2.3. Current Market Situation

As exposed by [24] most of the commercially available PVWPS systems uses either battery storage elements or DC motors (or both). The employment of a battery storage system allows extraction of maximum PV power, but its life span is approximately 2 years and the frequent need for replacement is a costly affair. Thus, a PVWPS with batteries would not suit the aimed solution by this work.

In [29] is presented a review of the PVWPS global trends and market opportunities. It was disclosed that an increasing number of solar water pump manufacturers, both startups and large established manufacturers, have entered the market. Their target resides on the adaptation of technology and business models to design and sell pumps suitable for a wider customer base. Therefore, the effect seen is that now more products tailored for smallholder farmers are available. It was reinforced that the upfront costs of PVWPS still higher than equivalent systems with diesel pumps - the average entry-level diesel pump starts at USD 200 compared to approximately USD 600 to 800 for a solar equivalent - but PVWPS have lower lifetime costs.

Locations that show the most promising growth of PVWPS market are regions on Asia and Africa. According to [29], the PVWPS market in sub-Saharan Africa is clearly nascent. Recent market surveys indicate that approximately 5000 solar water pumps were sold in sub-Saharan in the second half of 2018, of which over 3000 were sold in East Africa.

The decrease on PV technologies prices and increased numbers of market players have granted a decrease in the price of PVWPS, with prices falling by 80% over the past two decades [29]. Although, for many smallholder farmers and marginal population, solar powered water pumping remain unaffordable. The price of a small-scale pump is equivalent to at least 6-12 months' income for a typical farming household [29]. A variety of incentives are needed to stimulate the PVWPS market to reach scale. These incentives shall come from government policies; innovative financing; technology and product adaptation; and partnerships among various stakeholders.

**Figure 12** shows three different types of solar water pumping kits sold on market. It can be seen that PVWPS kits are available in power ranges from approximately 100W to 3750W. The prices are shown in US dollars and correspond to a calculated average according to what was found on the market.

| | SUBMERSIBLE PUMP - LARGER | SUBMERSIBLE PUMP - MICRO | SURFACE PUMPS |
|---|---|---|---|
| |  |  |  |
| **DESCRIPTION** | Fixed pump and PV panels, tailored installation | Semi-fixed pump and PV panels, guided installation | Mobile pump and PV panel, guided installation |
| **TECHNICAL SPECS** | 3-5 HP. Maximum suction lift of 350m | Works on a 160-260W panel, with a flow rate of up to 3,000 liters/hr. Maximum suction lift of 65 meters. | Works on an 80-120W panel, with a flow rate of up to 3,600 liters/hr. Maximum suction lift of 7 meters. |
| **STARTING PRICE (BRANDED)** | 3,500 USD | 650 USD | 695 USD |

**Figure 12:** Types PVWPS kits currently available on market [29].

The most common use for solar water pumps is as part of irrigation systems. But a study held on East Africa found that 22% of solar water pump customers do not use their pumps for farming. It is seen the use of PVWPS for domestic or small-scale commercial use (water sources for schools; places of worship; construction sites; etc.). In India it is also seen the use of solar pumps for household water rather than farming [29].

The use of PVWPS for household water has a positive impact particularly on women, who tend to be responsible for collecting water for the house needs. Also, as exposed by [29], in South Asia and sub-Saharan Africa, women are part of almost 50% of the agricultural labor force and are more likely to farm fruits and vegetables - cultivation that can highly benefit from irrigation. The use of PVWPS could reduce the time and effort women spend tending these crops.

In terms of the PVWPS manufacturers, there are companies based in China and Taiwan that produce solar water pumps and related equipment targeting the lowest cost market, with limited installation and technical support. Their products are being distributes widely across sub-Saharan Africa and India [29]. The low price of these products is their main selling point for farmers and marginal population.

Most branded products of PV water pumping on the market work only with their manufacturer's own equipment. As an example, can be cited the equipment sold by Grundfos. Among the equipment are solar inverters with MPPT (2.2-37kW), three-phase AC submersible motor-pumps and a water ATM (Automated Teller Machine). **Figure 13** shows a part of Grundfos' portfolio. The equipment available are embedded with a technology that it is either too expensive for costumers with limited purchasing power or have limited applicability (working only with the company's own products). Also, the

company does not provide solutions for low power applications, such as installations of 1kW maximum.

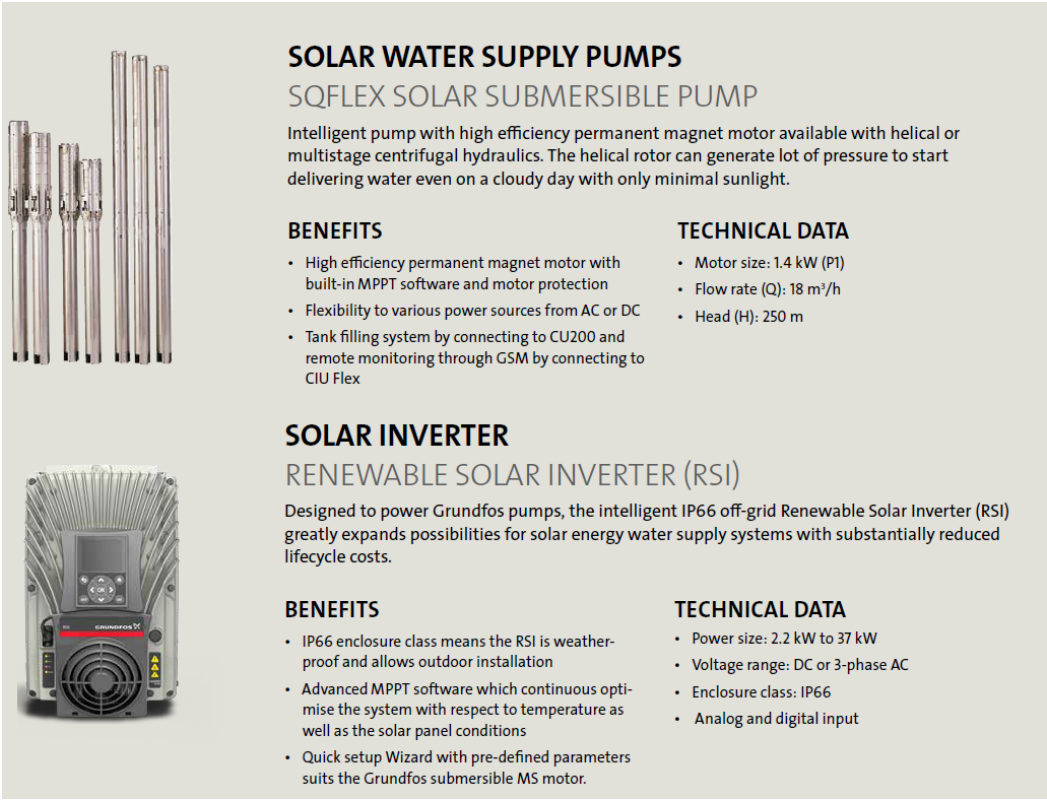


**Figure 13:** Grundfos' solar water pumping equipment. Image from [30].

If companies focus on improving the compatibility of PVWPS equipment, in order to integrate their own products with other manufacturers' equipment, they will see great potential into market penetration. The manufacturers can only benefit from creating solar water pumping equipment that can be modular as well as integrate the existing PV systems – the ones present in houses and industries.

# 3. Proposed Solution for Low Power PVWPS

After some meetings with VALLED representatives, in which it was discussed about possible layouts of PVWPS, the company presented the designed structure that meets the installation needs of customers like the Angolan government.

**Figure 14** presents the structure designed by VALLED. The structure can lodge up 4 PV modules as well as semi-cylindrical water tanks. The system shall operate with a submersible water pump of 1 HP that can either be single or three-phase, depending on the SFC that will be employed.

**Figure 14**: PVWPS structure designed by VALLED. Image provided by the company.

According to what was exposed, the role of this work is to propose a PVWPS composed by equipment that suits the requirements. Therefore, this section suggests a few solutions for low power PVWPS and presents the chosen voltage step-up DC-DC converter. The suitable equipment, such as possible PV modules, SFCs and water pumps are described.

## 3.1. Suggested Systems

Research has led to a few single-phase input/output frequency converters, which would be appropriate to run conventional single-phase AC motor-pumps. SFCs with three-phase output are the majority on market.

The desired characteristics that an SFC should have in order to compose solutions for low power solar pumping are: being cost-effective and with simple structure; being available in a power range from 1-2HP; presenting an internal PI controller; having at least one analog signal input and output, which can be configured to obtain a voltage or current signal (0 - 10V or 4 - 20mA). **Table 1** presents several alternatives of frequency converters that could be considered for the desired solution.

**Table 1:** Frequency converters suggested to be employed in the low power PVWPS solutions.

| Manufacturer | Model | Input | Output | Description | Price[1] |
|---|---|---|---|---|---|
| ABB | ACS255-01x-04A3-1 | 1-phase / 110-120$V_{ac}$ | 3 Phase / 200-240$V_{ac}$ / 4.3A / 1HP | GP[2] drive; PI Control. | 350€ |
| | ACS355-01x-04A7-2 | 1-phase / 200-240$V_{ac}$ | 3-phase / 200-240$V_{ac}$ / 4.8A / 1HP | Drive for AC IM and PMSM; undercurrent protection; PID Control . | 260€ |
| | ACS150-01x-04A7-2 | | | GP[2] drive; PID Control. | 145€ |
| Control Techniques | Commander C Cx00-021 | 1-phase / 100-120$V_{ac}$ | 3-Phase / 240$V_{ac}$ / 4.2A /1HP | GP[2] drive; PID Control. | Not found |
| | Commander C Cx00-012 | 1-phase / 200-240$V_{ac}$ | | | 211€ |
| Danfoss | VLT® Micro Drive FC51 - PK75 | 1-phase / 200-240$V_{ac}$ | 3 Phase / 240$V_{ac}$ / 4.2A / 1HP | GP[2] drive; PI Control. | 190€ |
| Invertek | Optidrive E3 ODE-3-120070-1012 | 1-phase / 200-240$V_{ac}$ | 1-phase / 200-240$V_{ac}$ / 1HP | GP[2] drive; PI control. | 330€ |
| Salicru[3] | CV30-008-S2 PV | 200-400$V_{dc}$ / 330$V_{MPP}$ | 3 Phase / 240$V_{ac}$ / 4.2A / 1HP | PV water pump drive; MPPT; PID control. | 250€ |
| Schneider | ATV12H075F1 | 1-phase / 100-120$V_{ac}$ | 3-phase / 200-240$V_{ac}$ / 4.2A / 1HP | GP[2] drive; PID control | 144€ |
| Italtecnica[3] | SIRIO ENTRY | 1-phase / 230$V_{ac}$ | 1-phase / 230$V_{ac}$ / 10.5$A_{max}$ / 2HP max | Motor-pumps drive; PID Control. | 467€ |
| WEG | CFW10 | 1-phase / 200-240$V_{ac}$ | 3-phase / 200-240$V_{ac}$ / 4.2A / 1HP | GP[2] drive; PID control. | 175€ |
| YASKAWA | J1000 Series BA0006 | 1-phase / 200-240$V_{ac}$ or 260-340$V_{dc}$ | 3-phase / 200-240$V_{ac}$ / 5A / 1HP | GP[2] drive; V/f PI control. | 160€ |

[1] Average of prices from various websites; [2] GP = general-purpose; [3] Dedicated water pump drivers.

All the prices of the equipment listed on **Table 1**, **Table 2** and **Table 3** were found through a brief search on the internet and may not represent the prices that a legal-entity would get when negotiating with the manufacturer.

In the scope of the motor-pumps, it was chosen the submersible ones driven by AC induction motors. Preference was given to the well-stablished manufacturers on the market and the ones that are already reliable suppliers of water pumps to VALLED. **Table 2** presents the suggested water pumps.

**Table 2:** Water pumps suggested to be employed in the low power PVWPS solutions.

| Manufacturer | Model | Description | Price[1] |
|---|---|---|---|
| Ideal Delta | B-21/17i/F | 1-phase / 230$V_{ac}$ / 1HP / 50Hz / 2.6m³/h | 453€ |
| Wilo | TWI4.10-15.10 / 2-wire motor | 1-phase / 230$V_{ac}$ / 1HP / 60Hz / 2.3m³/h | 592€ |
| | TWI4.10-15.10 / 3-wire motor | 3-phase / 230$V_{ac}$ / 1HP / 60Hz / 2.3m³/h | 639€ |

[1]Average of prices from websites.

Regarding the photovoltaic modules, the choice was based on the ones sold by the most popular manufacturers, as well as the ones from companies that VALLED already purchase. Among these manufacturers can be cited Canadian Solar, Sun Power, Panasonic and REC. PV technology is well established and the majority of conventional PV modules from distinct manufacturers have similar voltage x power characteristics. **Table 3** presents PV modules that can be employed in low power PVWPS.

**Table 3:** PV modules suggested to be employed in the low power PVWPS solutions.

| Manufacturer | Model | Electrical Specifications[1] | Size | Price[2] |
|---|---|---|---|---|
| Sun Power | SPR-E19-320 | 54.7$V_{MPP}$ / 320W | 1558 x 1046 x 46mm | 304€ |
| Panasonic | VBHN325SA16 | 57.6$V_{MPP}$ / 325W | 1590 x 1053 x 35mm | 297€ |
| REC | REC300PE72 | 36.4$V_{MPP}$ / 300W | 1968 x 991 x 45mm | 204€ |
| | REC275PE | 31.5$V_{MPP}$ / 275W | 1665 x 991 x 38mm | 120€ |
| Fluitecnik | FTS-220P | 29.38 $V_{MPP}$ / 220W | 1653 x 980 x 45mm | - |

[1]All the values described were taken from the modules' datasheets provided by the manufacturers. The data are from the modules operating at the STC (standard test conditions: irradiance=1000W/m²; cell temp.=25°C).

[2]Average of prices from websites.

Four distinct low power PVWPS layouts were presented to the company VALLED, they are shown in the sequence. The suggested layouts were composed according to the equipment presented on previous **Tables 1, 2 and 3**. The use of a maximum of 4 PV modules was considered (≈1m width conventional ones), due to the fact that the structure presented by VALLED (**Figure 14**) was designed for lodge that number of modules. Also, it was foreseen the use of either single-phase or three-phase 1HP submersible water pumps.

The Solution 1 is presented in the **Figure 15**. It was composed considering the use of only three PV modules for the water pumping system, thus, the left module would be available for powering another system that the structure (**Figure 14**) might lodge, such as lighting. The solution involves the use of a three-phase 230V submersible water pump and general-purpose frequency converters that contains an internal voltage boosting stage. The employment of these SFCs must be studied to verify if a DC input is possible and if, in this case, the voltage boosting stage would work.

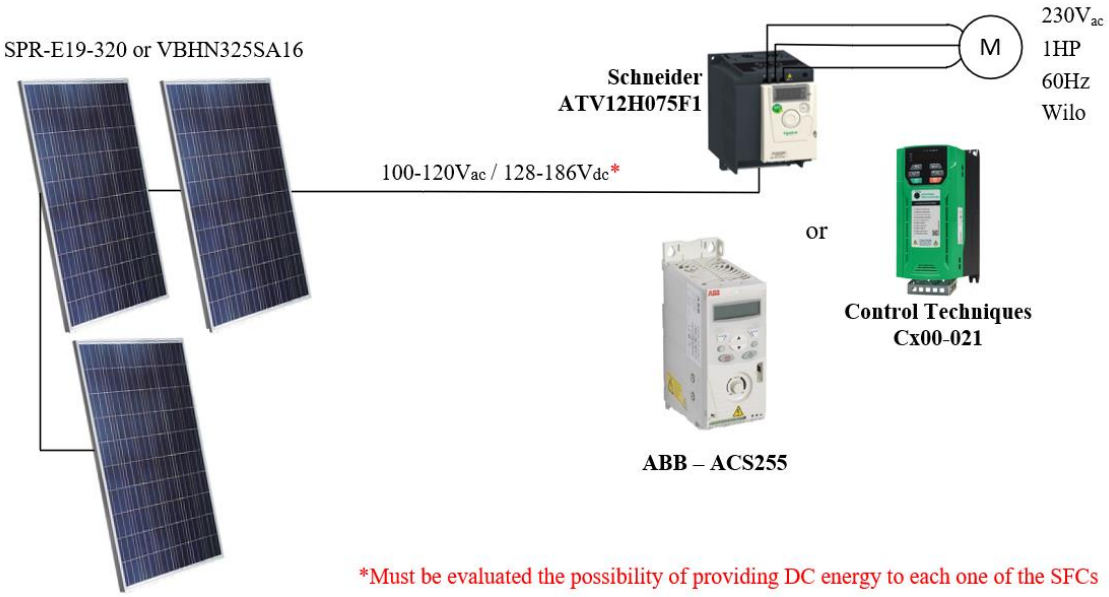


**Figure 15:** Solution 1 for low power PVWPS.

The Solution 2 is presented in the **Figure 16**. It was also composed with the intention that only three PV modules would be used for the water pumping system and the remaining one would power another equipment. The solution employs a DC-DC step up converter and a frequency converter properly built for PV water pumping. The DC-DC step-up converter is explained in the next Section 3.2. The chosen frequency converter

is from Salicru, a Spanish company. This equipment was selected because it is cost-effective when comparing to the others frequency converters (see **Table 1**); it is embedded with MPPT and PID controller; it presents over-voltage protection; it can detect dry well and full tank; and it can automatically start and stop depending on solar radiation. The chosen water pump is the 3-phase one from Wilo, presented in the **Table 2**. An equivalent water pump can be employed (three-phase / $230V_{ac}$ / 1HP), with operating frequencies of 50Hz or 60Hz.

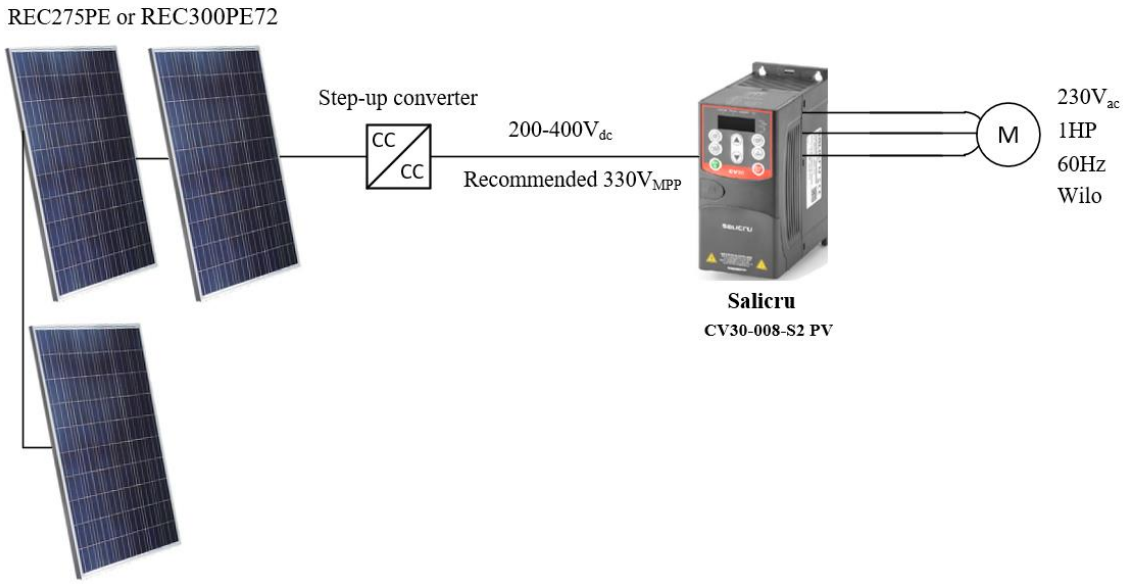


**Figure 16:** Solution 2 for low power PVWPS.

**Figure 17** presents the Solution 3. It was composed considering the possibility of using three or four PV modules for the water pumping system. The solution also employs a DC-DC step-up converter for boosting the input voltage in order to not oversize de PV panel (i.e. use just a number of PV modules needed to supply the required power) .

Two choices of single-phase input/output frequency converters are presented for the Solution 3. One is from Invertek and it is an SFC for general-purposes application. The other one is from Italtecnica and it is a frequency converter properly built for water pumping, thus, have some features like the protection against dry running. This Italtecnica frequency converter is the most expensive among the converters found but it was proposed for the company VALLED so that they can do a better price search and, perhaps, obtain a great offer.

The suitable water pump for composing Solution 3 must be single-phase 230$V_{ac}$ of 1HP. It can be either 50Hz or 60Hz. There is flexibility in choosing water pumps of these frequencies because SFCs can operate both.

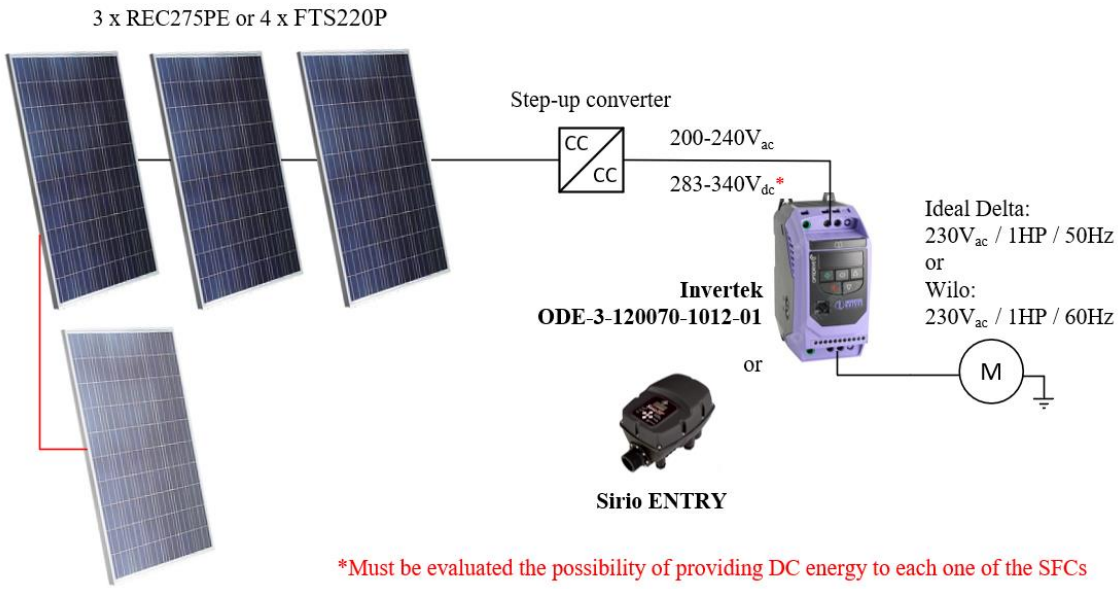


**Figure 17:** Solution 3 for low power PVWPS.

The last solution presented is shown in the **Figure 18**. Solution 4 employs the most common type of SFCs among the selected ones. The 3-phase output/230$V_{ac}$ SFCs were the majority found on the market, considering SFCs that would suit the desired low power PVWPS solution.

The layout proposal for the Solution 4 is to employ either three or four PV modules, such in Solution 3. It was also considered the use of a DC-DC step-up converter to boost the voltage levels of 90-110$V_{dc}$ to 283-340$V_{dc}$. SFCs manufactured by the main companies on the market, like ABB and WEG, can be used. The water pumps that can be employed are the 3-phase/230$V_{ac}$ ones like the TWI4.10-15.10/3-wire from Wilo.

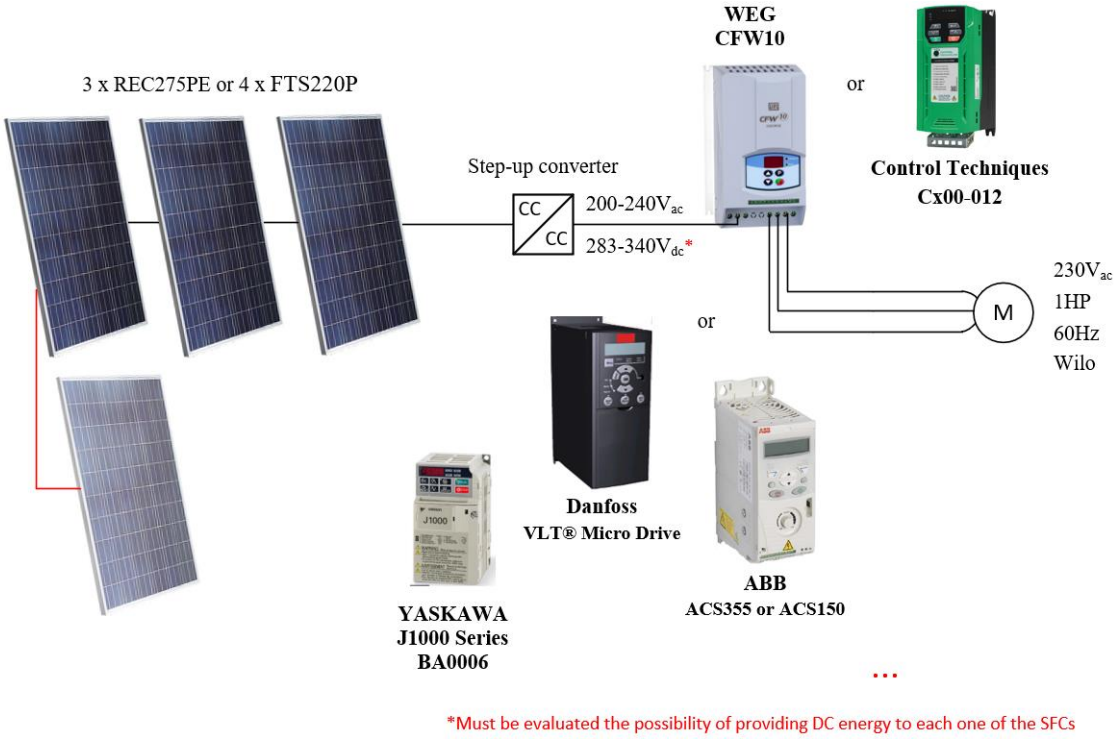


**Figure 18:** Solution 4 for low power PVWPS.

### 3.2. Step-up Converter

The employment of a voltage step-up converter on a low power PVWPS has proven to be significant. When choosing an electronic converter topology, one has to keep in mind on what are the indispensable characteristics of the desired module. In the case of this work, the designed converter has to be robust and simple; based on components widely available on the market; cheap; with control circuit that provides an output voltage limitation and an optimized input voltage configuration (with the set-point given by an MPPT electronic circuit).

PV modules have characteristic of low energy conversion efficiency (up to 21%). Thus, the maximum energy should be extracted from the PV module for a great PV system operation. There is only one maximum power point (MPP) for a solar panel and it varies with climatic conditions, such as irradiance and temperature. Usually the tracking of the MPP is implemented in the DC-DC converters circuit, by an MPPT algorithm. In this ambit, commonly used DC-DC converters are Buck, Boost, Buck-Boost, Cúk and SEPIC [27].

DC-DC converters can either be current-fed or voltage-fed. This last type of converter is not the best choice for PV water pumping application [17]. Current-fed

converters have some advantages when compared to the voltage-fed topologies. Those ones generally have an inductor at the input, so the system can be dimensioned to have the input current ripple as low as necessary, thus eliminating the need for an input capacitor (used to prevent the PV panel suffer from the current ripple). Current-fed converters are normally derived from the Boost converter [17].

The conventional Boost converter can provide, with acceptable efficiency, an output voltage gain only about 2 to 3 times the input voltage, so, this converter may not suit well the aimed solution of this work. Other current-fed DC-DC converters like Cúk and SEPIC have higher voltage gains and may be more efficient in applications involving PV modules [27]. They provide a high voltage-boosting capacity, which helps to reduce the required transformation rate of the transformer (if applied). Additional topologies that can be cited are the current-fed push pull converter, current-fed full-bridge and the dual half-bridge converter. Although current-fed topologies have all the mentioned advantages, they still have problems with high voltage spikes created due to the dispersion inductance of the transformers [17].

A complete review of the DC-DC voltage boosting techniques and topologies is exposed in [31]. It is shown that the demands for reliable, efficient, small-sized, and lightweight step-up DC-DC converters can be simply achieved by employing converters like: SEPIC, Cuk, and Zeta. Furthermore, when galvanic isolation is required, the flyback, forward, push-pull, half-bridge and full-bridge converters are well suited. Voltage multiplier cells, magnetic coupling, multi-stage and switched-capacitor are among the cited voltage boosting techniques [31]. **Figure 19** shows some of the cited DC-DC voltage step-up topologies.

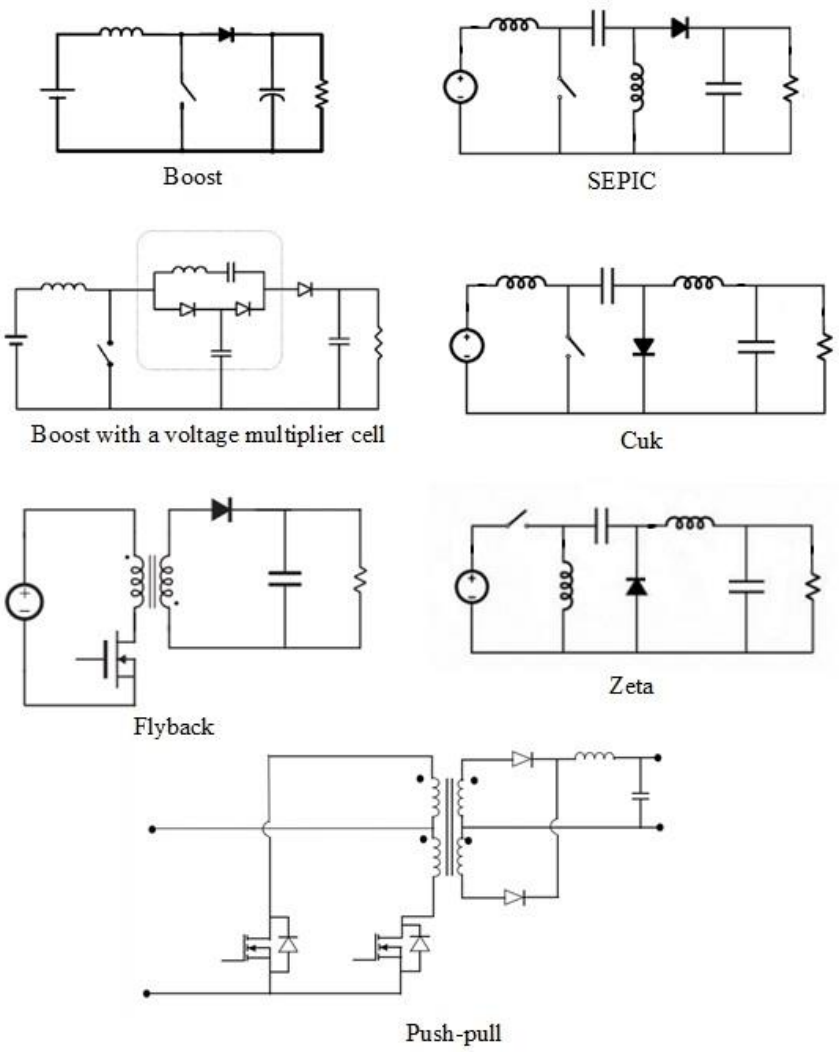


**Figure 19:** DC-DC converters step-up topologies. Image adapted from [31].

Among the aforementioned boosting techniques, the switched-capacitor is the one chosen to be considered in the designed step-up converter. The technique is based on a charge pump circuit, which is already employed in many converters. The voltage boosting in a charge-pump circuit comes only from capacitive energy transfer and does not involve magnetic energy transfer. Switched-capacitor approaches to circuit implementation are very popular due to their modularity characteristic [31].

The Switched-Capacitor Double Boost (SCDB) was the converter chosen to compose the afore presented PVWPS solutions. This topology was already addressed by [32] and the tests showed promising results. The converter is composed by an integration of the conventional Boost converter topology with a switched-capacitor stage. This integration is based on the addition of two capacitors (Cm and C2) and two diodes (D2 and D3). **Figure 20** shows the topology of the SCDB converter.

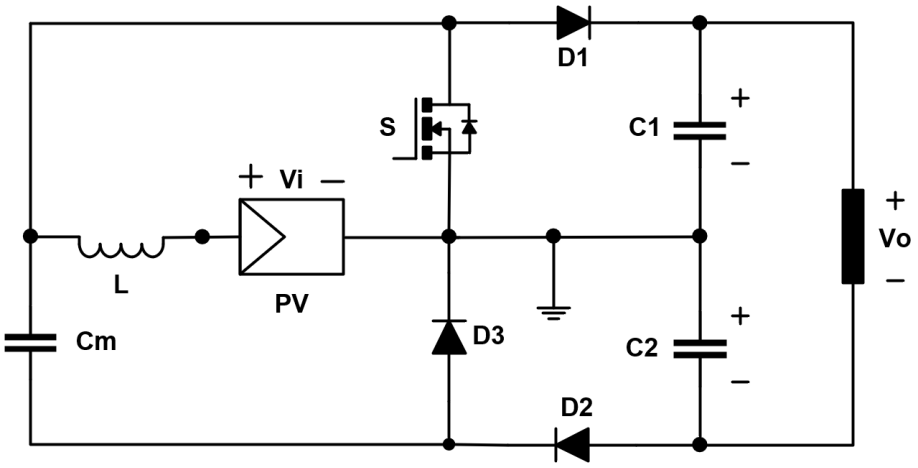


**Figure 20:** Switched-Capacitor Double Boost converter. Image adapted from [32].

In the SCDB converter the PV string reference is not the same as the output reference. Also, this is a solution with an output operating as a voltage source (such as boost), which leads to the use of larger capacitors at the output.

The integration of a switched-capacitor stage to the Boost converter makes it possible to obtain higher levels of voltage gain with the advantages of not adding semiconductors switches; not adding magnetic elements; and avoiding extreme duty cycle of the switch (which implies in efficiency loss). Adding switches to a topology leads to an increase in the complexity of drivers and control circuit. Also, magnetic elements usually are the largest and costly components of a converter, their use significantly impacts efficiency and reliability [33].

If the conventional Boost topology had been chosen, the voltage requirements of the suggested systems would imply in the use of an IGBT switch or a 650V MOSFET (typical value). By using an IGBT, the switching frequency would be limited to a maximum of 30kHz, which would lead to a larger inductor.

### 3.2.1. Operating Stages and Equations

The main equations necessary for design the SCDB converter can be deduced by analyzing its operating stages. It will be considered that the converter will operate at a continuous current mode (CCM), which means that the current in the inductor never goes to zero. This is a consideration because it is desirable that the input current ripple (PV current) does not present a too high value. As exposed by [32], when operating in CCM the SCDB converter has two stages of operation.

The **Figure 21** presents the stage in which the switch S is closed (switched on). In this stage the inductor (L) is charged with the energy provided by the PV panel at the same time that capacitor Cm discharges on capacitor C2. Also, if the capacitor C1 has energy, it is transferred to the load. The diodes D1 and D3 are inversely polarized, therefore do not conduct electric current. The reverse voltage that each one of the diodes must withstand is approximately half the output voltage $V_o$.

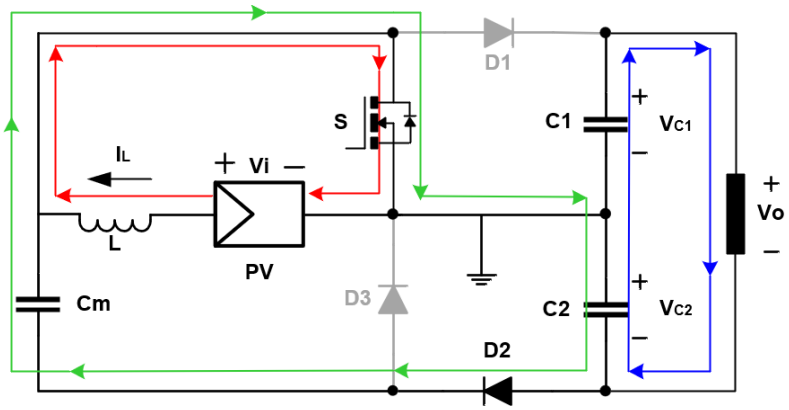


**Figure 21:** SCDB converter operating stage when S is switched on. Image adapted from [32].

The next stage of operation is presented in the **Figure 22**. When the switch is turned off (S is open), the energy stored in L is transferred to C1. This is what also would happen if the converter topology were the conventional Boost one. The difference is that in the SCDB converter there is another capacitor (C2) that was previously charged, thus, in this stage it discharges on the load. The switched-capacitor Cm that had been discharged in C2 at the first stage, now it is charged by the energy from the PV panel.

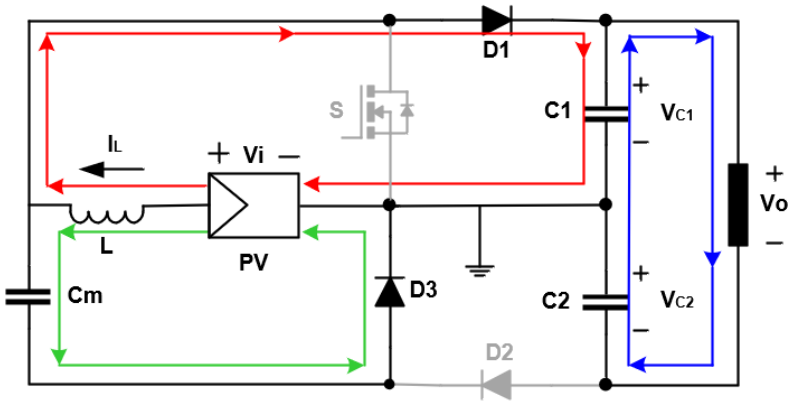


**Figure 22:** SCDB converter second operating stage - S switched off. Image adapted from [32].

The value of the voltage across C1 plus the voltage drop in the diode D1 is the voltage stress that the switch S must support when it is turned off. In this second stage of operation, the diode D2 is inversely polarized and it must support a voltage stress of approximately half of the total output voltage, that is the voltage across C1 plus the voltage drop in the diode D3.

The equation and dimensioning of the SCDB is similar to the conventional Boost converter, which was presented in [7]. The difference is that the SCDB converter provides a double voltage gain in comparison to the ordinary Boost.

The static gain of the proposed converter can be expressed by Equation 1, where $D$ is the duty cycle of the switch S, $V_i$ is the input voltage and $V_o$ is the output voltage.

$$\frac{V_o}{V_i} = \frac{2}{1 - D} \tag{1}$$

The well-known equation of the voltage across an inductor (Equation 2) can be used to calculate the minimum value of the inductor L, for guarantee CCM operation. The $\Delta I_L$ is the current ripple of the inductor; $L$ is the inductance value; $\Delta t$ is the time step; and $V_L$ is the voltage across the inductor.

$$V_L = L \cdot \frac{di}{dt} \quad \rightarrow \quad V_L = L \cdot \frac{\Delta I_L}{\Delta t} \tag{2}$$

Consider that $f$ is the switching frequency of S and $I_{MPP}$ is the maximum current provided by the PV panel (when operating at MPP). In the stage of operation where the inductor is being charged (**Figure 21**), $V_L$ is equal to the voltage of the PV string and the $\Delta t$ is equal to the duty cycle $D$ times the period of the switching time (1 / $f$). Also, one must have in mind that the maximum current ripple that L can have ($\Delta I_L$) is $I_{MPP}$. So, starting from Equation 2 and isolating $L$, the inductance value $L_{min}$ in order to guarantee CCM can be expressed by Equation 3.

$$L_{min} = \frac{V_i \cdot D}{I_{MPP} \cdot f} \tag{3}$$

The capacitance of the output capacitors ($C_1$ and $C_2$) can be calculated considering a predetermined value for their voltage ripple ($\Delta V_c$) using the well-known equation for the current through a capacitor Equation 4.

$$I_C = C\frac{dv}{dt} \quad \rightarrow \quad I_C = C\frac{\Delta V_c}{\Delta t} \tag{4}$$

As can be seen in the **Figure 21**, in the period of time that S is closed ($D \cdot 1/f$) the current through the capacitor $C_1$ is the total output current $I_o$ (load current). It is considered that capacitors $C_1$ and $C_2$ will have the same capacitance, to facilitate the design of the converter and the voltage balance. So, the minimum capacitance $C$ to ensure the desired voltage ripple $\Delta V_C$ can be expressed by the Equation 5.

$$C_1 = C_2 = C = \frac{I_o \cdot D}{\Delta V_C \cdot f} \tag{5}$$

To predict a value for capacitor $C_m$ it is needed a more complex analysis. Results of experimental tests performed with an SCDB converter, exposed by [32], showed that a value for $C_m$ capacitance ten times smaller than the capacitance of $C_1$ and $C_2$ provides a correct operation of the converter.

As it was already seen, in the SCDB converter the voltage across the switch S is approximately the half of the total output voltage. Considering an ideal circuit, the voltage that S must support ($V_S$) is expressed by Equation 6.

$$V_S = \frac{V_o}{2} \tag{6}$$

The SCDB converter switch is submitted to the half of the Boost switch voltage value, if compared the voltage across the switch of a conventional Boost converter with the associate SCDB converter, considering both with the same static gain. Also, the duty cycle ($D$) of the SCDB converter switch is half of the value of the analog conventional Boost switch.

For the SCDB converter to be employed in the solutions presented in Section 3.1 it must be dimensioned according to the voltage and power requirements of the systems. The basic requirements are that the converter boosts a voltage of approximately $90V_{dc}$ to a maximum of $340V_{dc}$ and that present a power capability of 1HP (750W). The electrical characteristics of the SCDB converter are presented in the following **Table 4**.

**Table 4:** Electrical characteristics of the SCDB converter.

| Parameter | Designation | Value |
|---|---|---|
| Maximum Power | $P$ | 750W |
| Nominal Input Voltage | $V_i$ | 90V |
| Maximum Input Voltage | $V_{i-max}$ | 120V |
| Nominal Output Voltage | $V_o$ | 310V |
| Voltage Ripple Across Capacitors | $\Delta V_c$ | 0.1% |
| Maximum Input Current | $I_{MPP}$ | 7.3A[1] |
| Nominal Output Current | $I_o$ | 3.5A |
| Switching Frequency | $f$ | 100kHz |

[1]This value was determined according to an average of the MPP current among the suggested PV modules.

The frequency at which a magnetic element works determines its size and weight. The higher the frequency, the smaller an inductor/transformer needs to be. When designing an electronics module with intentions of turning it into a product, size and weight matters. So, it was chosen a switching frequency ($f$) of 100kHz for the switch S. This value is higher than the frequency at which other proposed converters for low power PVWPS operate, as the one presented in [7]. Also, after a brief search on the market, it was found some high frequency SMD inductors and a MOSFET that would suit the needs of the SCDB converter.

Considering the electrical parameters presented in the **Table 4**, the previous Equation 1 can be employed to calculate the static gain of the converter and the duty cycle of the switch S, respectively resulting in $V_o/V_i = 3.44$ and $D = 0.42$. Also, can be calculated the values for the minimum inductance and capacitances, as presented in the following **Table 5**.

**Table 5:** Calculation of the inductance and capacitances of the SCDB converter.

| Element | Designation | Calculation | Value |
|---|---|---|---|
| Inductor | $L_{min}$ | $L_{min} = \frac{90 \cdot 0.42}{7.3 \cdot 100k}$ | 51.78µH |
| Capacitor | $C_1$ | $C_1 = C_2 = \frac{3.5 \cdot 0.42}{0.01 \cdot {}^{310}/_{2} \cdot 100k}$ | 94.7µF |
| | $C_2$ | | 94.7µF |
| | $C_m$ | $C_m \cong {}^{C_1}/_{10}$ | 9.47µF |

### 3.3. Control

As exposed by [14], in systems fed by PV energy the voltage control is more effective. The **Figure 23** shows an example of an I x V curve for a PV module, it is indicated an approximately line for the maximum power point voltage according to irradiance levels. It can be seen that the $V_{MPP}$ of PV modules remains relatively constant in a wide range of irradiance variation while the current shows an expressive change. This behavior favors the choice of the voltage as the variable to be controlled. For this reason, voltage control in PV-driven systems is preferable than current control.

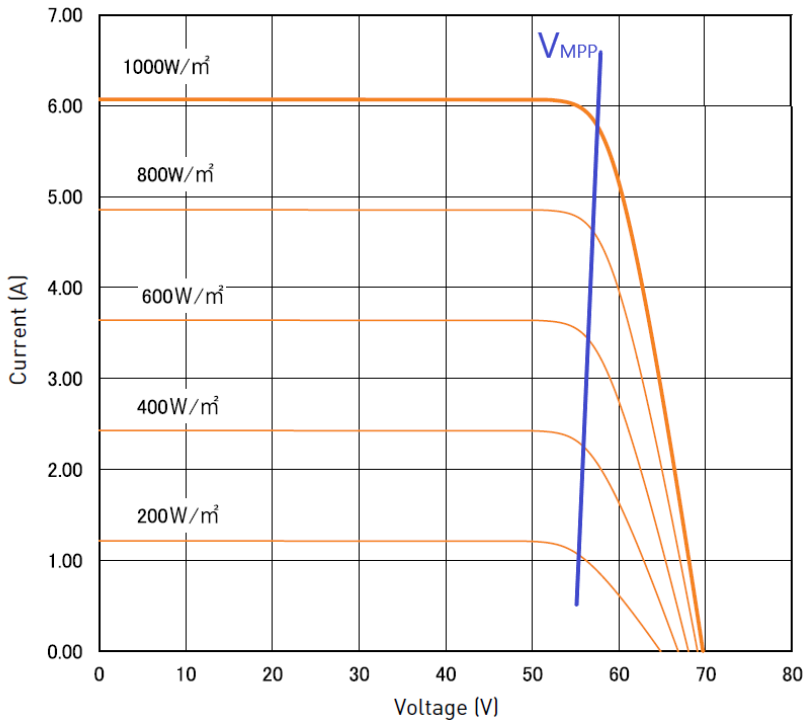


**Figure 23:** I x V curve of the PV module VBHN325SA16 (disponible in the datasheet of the module, provided by Panasonic).

The SCDB converter is designed to operate in systems with an SFC that contains PI/PID control (or even with frequency converters already embedded with MPPT). So, the frequency converter is the equipment responsible for regulating the operation of the water pump in situations of irradiance variations and partial shading. Considering this, for the SCDB converter application the Constant Voltage control technique is enough. This technique is not as efficient as the MPPT Perturb and Observe technique, but it suits well the requirements of the proposed systems.

When employing an SFC, its PI/PID controller will control the DC-link voltage around a preset value by varying the pump speed. **Figure 24** illustrates the PI control scheme of an SFC.

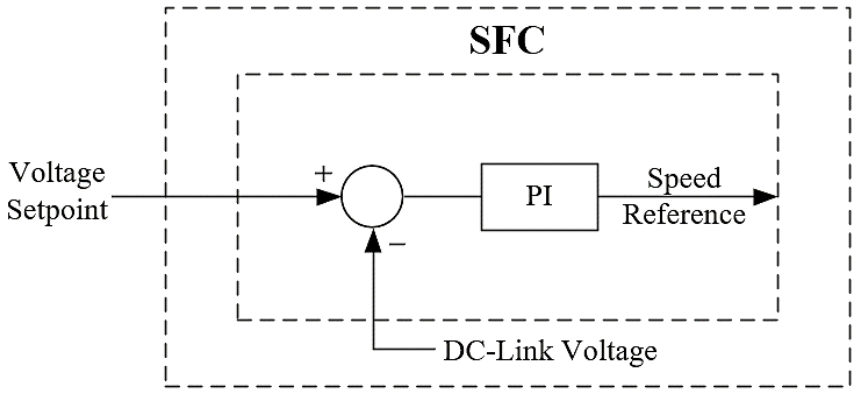


**Figure 24:** Scheme of the SFC PID control.

In this type of control system (**Figure 24**), the error signal, that corresponds to the difference between the voltage setpoint and feedback value (DC-link voltage) is introduced in the controller in order to change the frequency (speed) of the water pump. This change will maintain the DC bus voltage in the desired value despite the changes of the PV power provided.

The proportional gain (Kp) of the PI controller is responsible for minimizing the stationary error, inherent at any plant. Higher the Kp value, lower is the stationary error, but higher the oscillations and the required time for stabilization of the control variable. It means that an excessive value of Kp can unstable the process [34]. The effect of the integrative time (Ki) is to eliminate the stationary error. When the Ki value is large, the variable approaches the setpoint slowly. When Ki is small (which is an “over correction”),

the variable oscillates and takes more time to stabilize [34]. To ensure that the PVWPS operates properly, must be made a correct tuning of the SFC PI controller parameters.

The basic functions that the control circuit of the SCDB converter must present are an output voltage limitation and a capability to configure an optimum input voltage value, which can be made by a conventional PWM control. The need for an output voltage limitation is to protect the connected frequency converters in no-load situations (e.g. full tank). If a limitation is not imposed, the output voltage of the SCDB converter will be boosted beyond the limit of the components, until its fault.

The HW of the control circuit is presented in the Section 4.1 and its specific functions will be explained. The goal was to employ conventional components and compose a simple control module.

# 4. Hardware Validation

This section presents the hardware validation of the proposed step-up DC-DC converter. One of the solutions presented in Section 3.1 was also tested and validated. The equipment available in the LSE (Laboratory of Electromechatronics Systems) made it possible to test Solution 3 (**Figure 17**). The system is mainly composed by 3 PV modules, the Switched-Capacitor Double Boost Converter, an SFC and a submersible 750W water pump.

## 4.1. Switched-Capacitor Double Boost Converter

The dimensioning of the converter was presented on Section 3.2.1., where it were calculated the basic parameters for the power circuit stage. In Section 3.3 the control requirements were defined. The components selected for the assembly of the converter were the ones available in the laboratory and as similar as possible to the calculated values. **Table 6** presents the main components employed in the first prototype of the SCDB converter.

**Table 6:** List of components employed on the SCDB converter.

| Circuit | Component | Value / Ratings | Description |
|---|---|---|---|
| **Power Stage** | Inductor (L) | 100µH / $I_{SAT}$ = 9.4 A / $R_{DC}$ = 22.9mΩ | SMD High Current Inductor |
| | Capacitor Cm | 10µF / 250V | Polypropylene |
| | Capacitors C1 and C2 | 150µF / 250V | Electrolytic |
| | Capacitor Cin | 100µF /250V | Electrolytic |
| | Switch (S) | 200V / 50A | MOSFET IRFP260N |
| | Diodes (D1, D2 and D3) | $V_{RRM}$ = 1000V / $I_{FAVM}$ = 30A | DSEI 30-10A Fast Recovery Diode |
| **Control Stage** | Voltage Regulator | 1.25V to 125 V / 700mA | TL783 |
| | Electrolytic Capacitors | 10µF / 1µF / 47µF | Voltage Regulator Circuit |
| | CI PWM | 7V < Vcc < 40 $V_{REF}$ = 5V | TL494 |
| | Transistors | $V_{CBO}$ = 50V / $I_c$ = 100mA | BC547 and BC557 |
| | Potentiometers | 10kΩ / 0.5W | Precision – 25turns |
| | Resistors | 22Ω – 1MΩ | Comparators / driver / filter / regulator |
| | Ceramic Capacitors | 100nF | |
| | Capacitor CT | 1nF | $f = {}^{1}/_{CT \cdot RT}$ |
| | Capacitor RT | 10kΩ | |

The first lab-model of the SCDB converter was assembled according to the schematics presented in the **Figure 25** and its HW is shown in the **Figure 26**. For the PCB design it was used the software EAGLE.

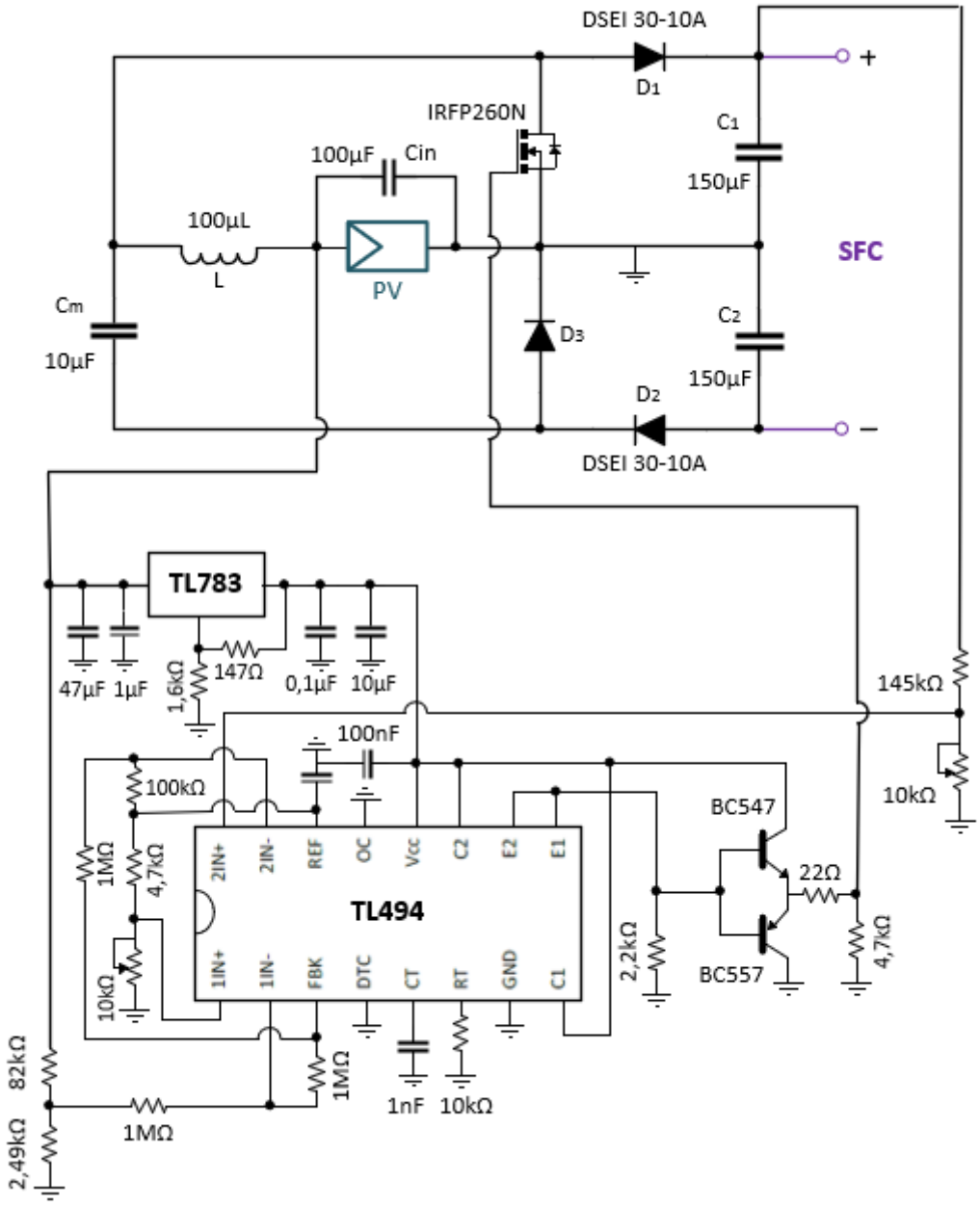


**Figure 25:** Schematics of the Switched-Capacitor Double Boost Converter with closed-loop control.

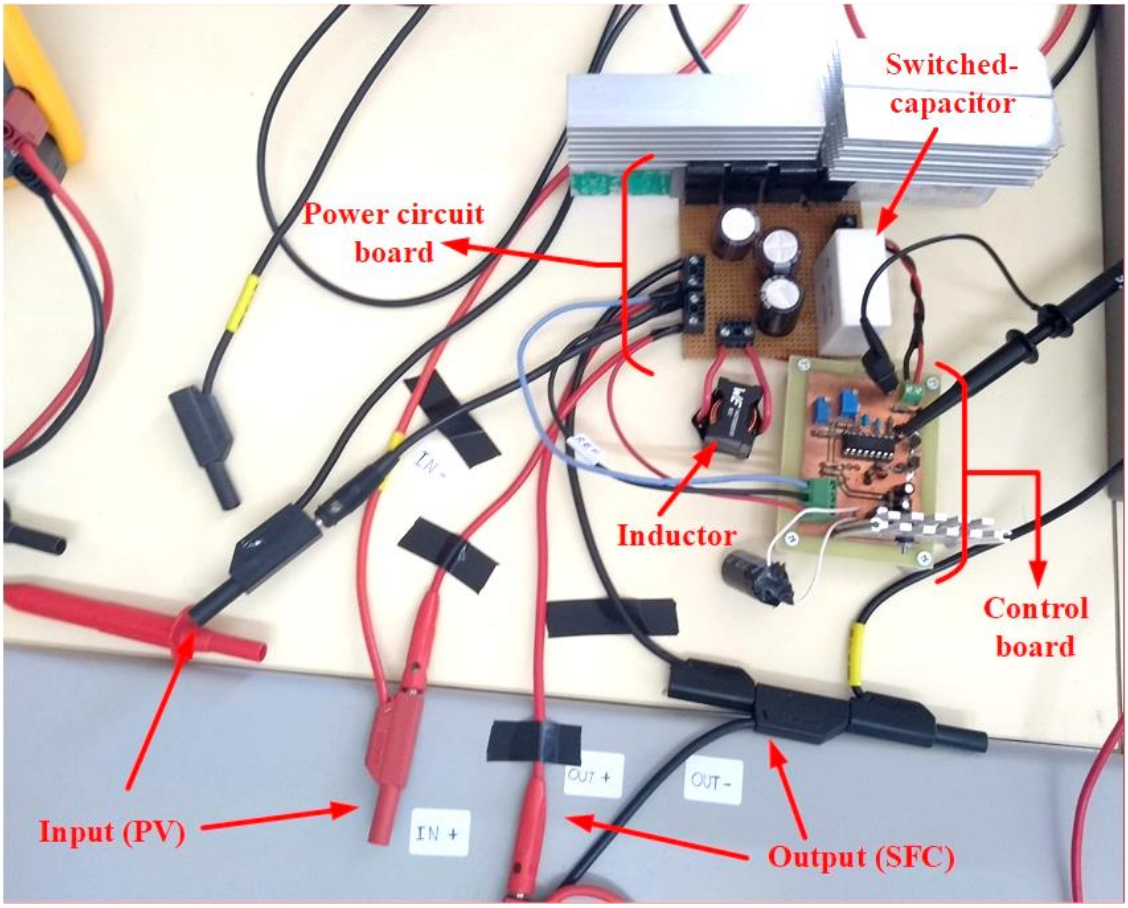


**Figure 26:** Switched-Capacitor Double Boost Converter HW implemented.

As it can be seen, the HW was divided into the Power Electronics board and the Control Circuit board. This separation was made to facilitate a possible change in the control circuit layout.

The power stage of the circuit employs three electrolytic capacitors: $C_1$ and $C_2$ at the output and $C_{in}$ at the input. The switched-capacitor $C_m$ is a polypropylene one, because it must be capable of operating at both polarity situations. The capacitor $C_{in}$ was employed to prevent the PV panel suffer from the current ripple caused by the input inductance. If the inductor has a higher inductance value, the current ripple will be reduced. Due to a market-availability limitation, the inductor was chosen basically respecting the minimum calculated inductance ($L_{min}$) and the maximum input current of the converter.

The initial goal was to propose a simple, feasible and cost-effective step-up converter, for companies like VALLED to be able to turn it into a product. Therefore, the SCDB converter was designed with a control circuit composed by conventional and well-known components, such as the PWM controller TL494 and the TL783 voltage regulator.

The implemented control circuit is similar to the one of the Boost converter presented by [7].

The TL783 is an adjustable three-terminal high-voltage regulator, with an output range capability from 1.25V to 125V. It is designed for high-voltage applications where standard bipolar regulators cannot be used [35]. The TL783 was employed to supply 15V to the control circuit of the SCDB converter. Using this component results in a limitation of the PV panel voltage, which cannot be higher than 125V. Thus, it must be payed attention to the numbers of PV modules used and their voltage.

Another component employed in the control circuit is the TL494. It is a Pulse Width Modulation (PWM) controller. It contains two error amplifiers, an on-chip adjustable oscillator, a dead-time control (DTC) comparator, a pulse-steering control flip-flop, a 5-V/5%-precision regulator and output-control circuits [36]. The simplified block diagram of the TL494 is shown in the **Figure 27**.

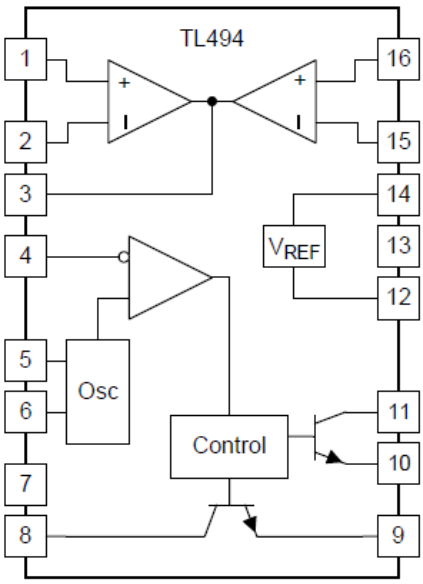


**Figure 27:** TL494 block diagram [36].

The first control function of the TL494 is responsible for imposing the input voltage (PV string voltage) by defining a suitable setpoint. This is performed through the configuration of the potentiometer connected to 1IN+ (see **Figure 25**). A change in the setpoint (potentiometer) will result in a change of the switch duty cycle, which will cause an increase or decrease of the power that can be extracted from the PV panel. The setpoint

must be configured in the moment of the PVWPS installation, considering the MPP voltage that the PV panel presents at the best days of irradiance in the location.

The second function of the control circuit is to limit the output DC voltage, protecting the frequency converter. Limiting the voltage across capacitor $C_1$ will result in a limitation of the capacitor $C_2$ voltage. The limitation of the voltage across capacitor $C_1$ can be configured by adjusting the potentiometer connected to the 2IN+ pin of the TL494 (see **Figure 25**). The adjustment must be made according to the maximum input voltage of the employed SFC (and respecting the maximum values of the components used). The controller will read the voltage across $C_1$ and compare to the setpoint (which is half of the maximum total output voltage), when that one reaches the limit value, the duty cycle of the switch is put to zero (or almost zero), so that it is stopped the voltage boosting.

### 4.2. SFC

The SFC used on the tests was the Invertek Optidrive E3, which was one of the suggested frequency converters (see **Table 1**). Its electrical specifications are shown in the **Table 7**. The Invertek SFC have an embedded PI controller, that is the PI Macro feature, which can be enabled and configured throughout the parameters.

**Table 7:** Invertek Optidrive E3 (ODE-3-120070-1012-01) technical specifications.

| **Electrical Parameter** | **Value** |
|---|---|
| Supply Voltage | 200-240$V_{ac}$ |
| Input Phases / Output Phases | 1 / 1 |
| Supply Current Continuous | 9.3A |
| Motor Output Rating | 1HP |
| Output Voltage | 0 – Supply Voltage (264$V_{ac}$ maximum) |
| Output Current (maximum) | 7A |

The Invertek SFC specification indicates that its nominal input voltage range is from 200$V_{ac}$ to 240$V_{ac}$, which are the RMS voltage values. It means that, the nominal voltage range required by the DC-link, after the rectifier stage, is 283-340$V_{dc}$. This value

is calculated by multiplying the nominal AC voltage range by the square root of two (e.g. $200V_{RMS} \cdot \sqrt{2} = 282.84V_{peak} \therefore 282.84V_{dc}$).

When choosing to operate the Invertek drive using the PI Macro feature the function of the digital and analog inputs are the ones presented in the **Figure 28**. It can be seen that the digital input 1 (DI1) is for enabling/disabling the output of the SFC and the digital input 2 (DI2) is for enabling/disabling an external PI reference, which is the DC-link voltage setpoint (see **Figure 24**).

| P-15 | DI1 | | DI2 | | DI3 / AI2 | | DI4 / AI1 | | Diagram |
|---|---|---|---|---|---|---|---|---|---|
| | 0 | 1 | 0 | 1 | 0 | 1 | 0 | 1 | |
| 0 | STOP | RUN | PI REF | P-20 REF | AI2 | | AI1 | | 5 |

**Figure 28:** Digital and analog inputs of Invertek Optidrive E3 when using Macro PI function (P-12 = 5 and P-15 = 0) [37].

The DC-link voltage setpoint can be configured by a potentiometer connected to the analog input 1 (AI1). The connection diagram of the Invertek SFC control terminals and its HW are presented in the **Figure 29**.

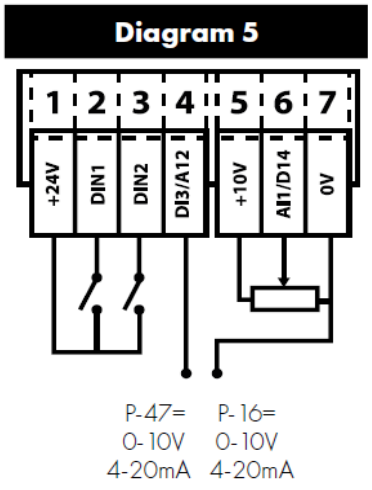



(a) (b)

**Figure 29:** (a) Invertek Optidrive E3 connections diagram [37] (b) HW connections.

In terms of the PVWPS protection, when using the Invertek Optidrive E3 one must have in mind that it presents just overload protection, as shown in the **Figure 30**. This overload protection trips when the current is higher than the set value, considering an extended period of time (e.g. 60 seconds). It is also possible to use a motor thermistor to trip the overload protection when the motor reaches a high temperature [37].

The drive has an in-built motor thermal overload function; this is in the form of an "I.t-trP" trip after delivering >100% of the value set in P-08 for a sustained period of time (e.g. 150% for 60 seconds).

***4.9.2. Motor Thermistor Connection***

Where a motor thermistor is to be used, it should be connected as follows:

| Control Terminal Strip | Additional Information |
|---|---|
| 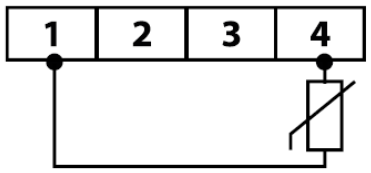  | Compatible Thermistor: PTC Type, 2.5kΩ trip level.<br>▪ Use a setting of P-15 that has Input 3 function as External Trip, e.g. P-15 = 3. Refer to section 7. Analog and Digital Input Macro Configurations on page 28 for further details.<br>▪ Set P-47 = "Ptc-th" |

**Figure 30:** Invertek Optidrive E3 overload protection [37].

The Invertek SFC has a configuration for Standby mode, as shown in the **Figure 31**. If this function is enabled, the SFC will enter in Standby (i.e. will disable its output) after a period of time of the motor running at its lowest frequency configured.

| | | | | | |
|---|---|---|---|---|---|
| **P-48** | **Standby Mode Timer** | **0.0** | **25.0** | **0.0** | **s** |
| | When standby mode is enabled by setting P-48 > 0.0, the drive will enter standby following a period of operating at minimum speed (P-02) for the time set in P-48. When in Standby Mode, the drive display shows StndbY, and the output to the motor is disabled. | | | | |
| **P-49** | **PI Control Wake Up Error Level** | **0.0** | **100.0** | **5.0** | **%** |
| | When the drive is operating in PI Control Mode (P-12 = 5 or 6), and Standby Mode is enabled (P-48 > 0.0), P-49 can be used to define the PI Error Level (E.g. difference between the setpoint and feedback) required before the drive restarts after entering Standby Mode. This allows the drive to ignore small feedback errors and remain in Standby mode until the feedback drops sufficiently. | | | | |

**Figure 31:** Standby Mode configuration of the Invertek Optidrive E3 [37].

In terms of under-voltage and other situations that might occur (e.g. DC bus ripple too high), the Invertek drive only presents warnings messages. The fault code messages that the SFC can display are presented in the **Figure 32**. For an example, when the voltage provided by the SCDB converter to the SFC runs at a lower value than its minimum voltage required, the U-volt (under voltage) message will be displayed. In this case, the user is responsible for manually turning the system off.

| Fault Code | No. | Description | Suggested Remedy |
|---|---|---|---|
| no-FLt | 00 | No Fault | Not required. |
| OI-b | 01 | Brake channel over current | Check external brake resistor condition and connection wiring. |
| OL-br | 02 | Brake resistor overload | The drive has tripped to prevent damage to the brake resistor. |
| O-I | 03 | Output Over Current | Instantaneous Over current on the drive output. Excess load or shock load on the motor. **NOTE** Following a trip, the drive cannot be immediately reset. A delay time is inbuilt, which allows the power components of the drive time to recover to avoid damage. |
| I_t-trP | 04 | Motor Thermal Overload (I2t) | The drive has tripped after delivering >100% of value in P-08 for a period of time to prevent damage to the motor. |
| PS-trP | 05 | Power stage trip | Check for short circuits on the motor and connection cable |
| O-uoLt | 06 | Over voltage on DC bus | Check the supply voltage is within the allowed tolerance for the drive. If the fault occurs on deceleration or stopping, increase the deceleration time in P-04 or install a suitable brake resistor and activate the dynamic braking function with P-34. |
| U-uoLt | 07 | Under voltage on DC bus | The incoming supply voltage is too low. This trip occurs routinely when power is removed from the drive. If it occurs during running, check the incoming power supply voltage and all components in the power feed line to the drive. |
| O-t | 08 | Heatsink over temperature | The drive is too hot. Check the ambient temperature around the drive is within the drive specification. Ensure sufficient cooling air is free to circulate around the drive. |
| U-t | 09 | Under temperature | Trip occurs when ambient temperature is less than -10°C. Temperature must be raised over -10°C in order to start the drive. |
| P-dEF | 10 | Factory Default parameters loaded | |
| E-trIP | 11 | External trip | E-trip requested on digital input 3. Normally closed contact has opened for some reason. If motor thermistor is connected check if the motor is too hot. |
| SC-Obs | 12 | Optibus comms loss | Check communication link between drive and external devices. Make sure each drive in the network has its unique address. |
| FLt-dc | 13 | DC bus ripple too high | Check incoming supply phases are all present and balanced. |
| P-LOSS | 14 | Input phase loss trip | Check incoming power supply phases are present and balanced. |
| h O-I | 15 | Output Over Current | Check for short circuits on the motor and connection cable. Note: Following a trip, the drive cannot be immediately reset. A delay time is inbuilt, which allows the power components of the drive time to recover to avoid damage. |

**Figure 32:** Fault code messages of the Invertek Optidrive E3 [37].

### 4.2.1. Parametrization

To parametrize the Invertek SFC, the installer has to know the technical specifications of the motor-pump that will be employed. Also, for correctly parametrizing the PI controller, it is necessary to know what the control variables are.

The DC-link voltage is the process variable controlled in a closed loop by the PI macro of the SFC. It is necessary to set the Proportional gain (Kp) and the Integrative time (Ki), which will determine the dynamic and steady-state error of the system, respectively. The measure of the DC-link voltage (PI control feedback) is internally given by the SFC and the reference value has to be set in a potentiometer or by a parameter (P-20), as seen in the previous **Figure 28**.

To address features like the V/f control or the PI macro of the Invertek SFC, the parameter P-14 must be set with a value equal to 101 so that the installer will have access to the parameter P-14 to P-60, which configurates those control features [37]. All the other main parameters of the Invertek Optidrive E3 are listed in the sequence:

- P-01 - Maximum Frequency / Speed Limit (Hz or RPM).
- P-02 - Minimum Frequency / Speed Limit (Hz or RPM).
- P-03 - Acceleration Ramp Time (seconds).
- P-04 - Deceleration Ramp Time (seconds).
- P-05 - Stopping Mode / Mains Loss Response: Selects the stopping mode of the drive, and the behavior in response to a loss of mains power supply during operation.
- P-07 - Motor Rated Voltage (Volts): 230 by default for the ODE-3-120070-1012-01.
- P-08 - Motor Rated Current (Amperes): This parameter should be set to the rated (nameplate) current of the motor.
- P-09 - Motor Rated Frequency (Hertz).
- P-10 – Motor Rated Speed: This parameter can optionally be set to the rated (nameplate) RPM of the motor. When set to the default value of zero, all speed related parameters are displayed in Hz and the slip compensation (where motor speed is maintained at a constant value regardless of applied load) for the motor is disabled.
- P-13 - Operating Mode Select (type of application).
- P-12 - Primary Command Source: Defines the control mode used, which defines how the motor will be controlled. The modes can be 0 - Terminal Control, 1 - Uni-directional Keypad Control, 2 - Bi-directional Keypad Control, 3 and 4 - Modbus Network Control, 5 - PI Control, 6 - PI Analog Summation Control, 7 and 8 - CAN Control or 9 - Slave Mode.
- P-15 - Digital Input Function Select: Defines the function of the inputs depending parameter P-12 (e.g. **Figure 28**).
- P-16 - Analog Input 1 Signal Format: Defines the format accepted by the terminal 6 (AI1). The options are: 0-10 V unipolar or bidirectional operation, 0-20 mA and 4-20 mA. These can also be reversed to operate with ranges such as 10-0V or 20-4 mA, for example.
- P-25 - Analog Output Function Select: Defines the functions of the analog output terminal, that can be either digital or analog. In the digital mode, one can select to output digital states such as if the drive is running, if the drive tripped, etc. If the output is chosen to be analog, the output signal

will reflect the chosen variable in a range from 0 to 10 V. The variables that can be selected are the motor speed, motor current, motor power or load current.

- P-30 – Start Mode, Automatic Restart, Fire Mode Operation: Parameter to set if the drive should start automatically if the enable input is latched during power on and how the automatic restart should work. If configured as “Auto-5”, the automatic restart delay is limited to 5 attempts with a 20 seconds interval.
- P-35 Analog Input 1 Scaling: The analog input signal level is multiplied by this factor, e.g. if P-16 is set for a 0 – 10V signal, and the scaling factor is set to 200.0%, a 5 volt input will result in the drive running at maximum frequency / speed (P-01).
- P-39 Analog Input 1 Offset: Sets an offset, as a percentage of the full scale range of the input, which is applied to the analog input signal. This parameter operates in conjunction with P-35, and the resultant value can be displayed in P00-01.
- P-41 - PI Controller Proportional Gain: Parameter to set the proportional gain of the PI control.
- P-42 - PI Controller Integral Time: Parameter to set the integral time of the PI Control.
- P-43 - PI Controller Operating Mode: Parameter to select how the PI control will work. There are four modes: 0 - direct operation; 1 - inverse operation; 2 - direct operation with wake at full speed; and 3 - inverse operation with wake at full speed. Direct operation means that, when the feedback signal drops, the motor speed increases and inverse operation that, when the feedback signal drops, the motor speed drops as well. The wake at full speed means that, when restarting from standby, the PI output is set to 100%.
- P-44 - PI Reference (Setpoint) Source Select: Parameter to set whether the PI reference source will be 1 - analog or 0 - digital. If analog, the reference is given by analog input 1.
- P-46 - PI Feedback Source Select: Parameter to set what will be the feedback source. The feedback can be 0 - analog input 1; 1 – analog input

2; 2 - motor Current; 3 - DC bus voltage; 4 - analog 1 – analog 2; or 5 - largest (analog 1, analog 2).

- P-47 - Analog Input 2 Signal Format: Defines the format accepted by the terminal 4 (analog input 2). The possible options are 0-10 V, 0-20 mA and 4-20 mA. This analog input can also be used with a motor thermistor.
- P-48 - Standby Mode Timer: Parameter to set how much time (in seconds) the SFC works with the minimum frequency before entering in standby mode.
- P-49 - PI Control Wake Up Error Level: Parameter to set the error of the PI to the SFC resumes normal operation after entering standby mode. This allows the SFC to only come back when there are enough conditions to it. The default value is 5%.

The main values of the parameters used on the tests are listed in the **Table 8**:

**Table 8:** Parameters of the Invertek drive used on tests.

| **Parameter** | **Value** | **Parameter** | **Value** |
|---|---|---|---|
| P-01 – Max. Frequency | 3100rpm | P-30 – Start mode | Auto-5 |
| P-02 – Min. Frequency | 2100rpm | P-35 – AI1 Scaling | 100% |
| P-03 – Acceleration Time | 5s | P-39 – AI1 Offset | 0 |
| P-04 - Deceleration Time | 5s | P-40 – Scaling Factor / Source | 0 / 3 |
| P-07 – Motor Rated Voltage | 230V | P-41 – PI Proportional Gain | Kp[1] |
| P-08 – Motor Rated Current | 3A | P-42 – PI Integral Time | Ki[1] |
| P-09 – Motor Rated Frequency | 50Hz | P-43 – PI Operating Mode | 1 |
| P-10 – Motor Rated Speed | 2900rpm | P-44 – PI Reference | 1 |
| P-12 – Command Source | 5 | P-46 – PI Feedback Source | 3 |
| P-15 – DI Function Select | 0 | P-48 – Standby Mode Timer | 0 |
| P-16 – AI1 Signal Format | U0-10 | P-49 – PI Wake Up Error Level | 5% |

[1]Each test performed employed different PI proportional gain and integral time values. They are shown in the next section.

### 4.3. Tests Conditions

The low power PVWPS tested was the one from Solution 3 presented on Section 3.1. Its basic scheme is shown in the **Figure 33**. The system was tested in a laboratory environment; with two types of PV modules; with a single-phase 750W/230$V_{ac}$ water pump; with an improvised hydraulic circuit; at different weather conditions; and with distinct PI control parameters of the SFC Invertek Optidrive E3.

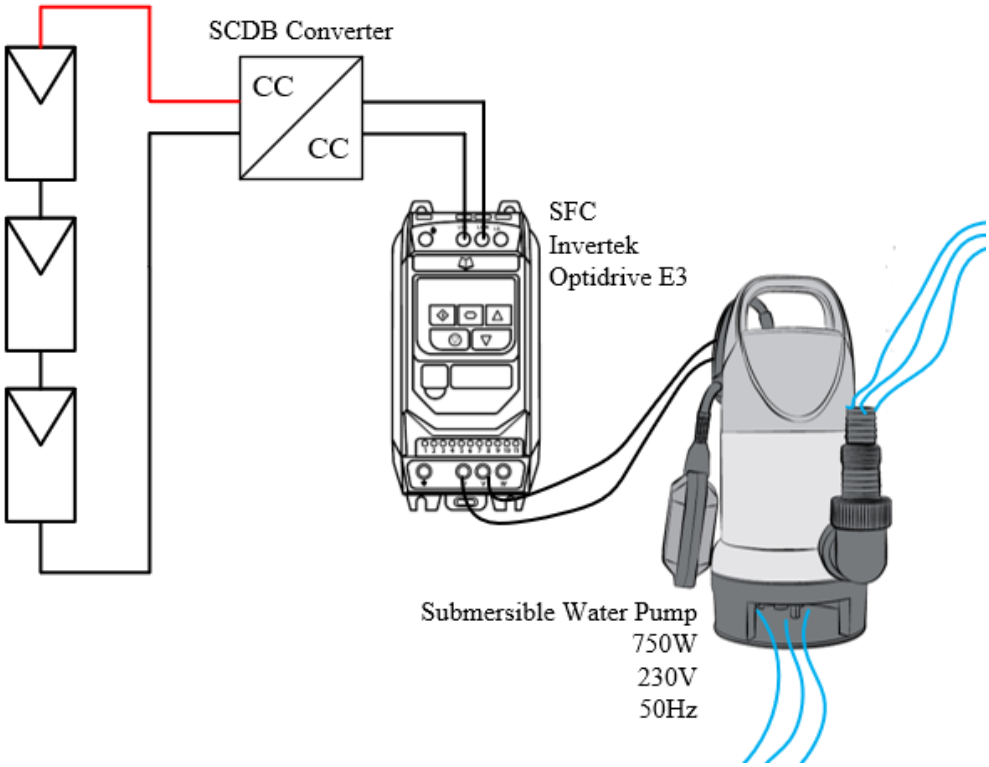


**Figure 33:** Scheme of the low power PVWPS tested system.

The experimental platform employed on the tests is shown in the **Figure 34**. The two PV strings employed can be seen in the **Figure 35**, the one with the Fluitecnik modules is lodge on the roof of ESTiG (IPB) building, in a static structure directed South and at a 35° inclination. The panel with the three REC modules was placed outside the LSE laboratory at approximately 40° inclination. Its direction could be modified to achieve better PV power generation.

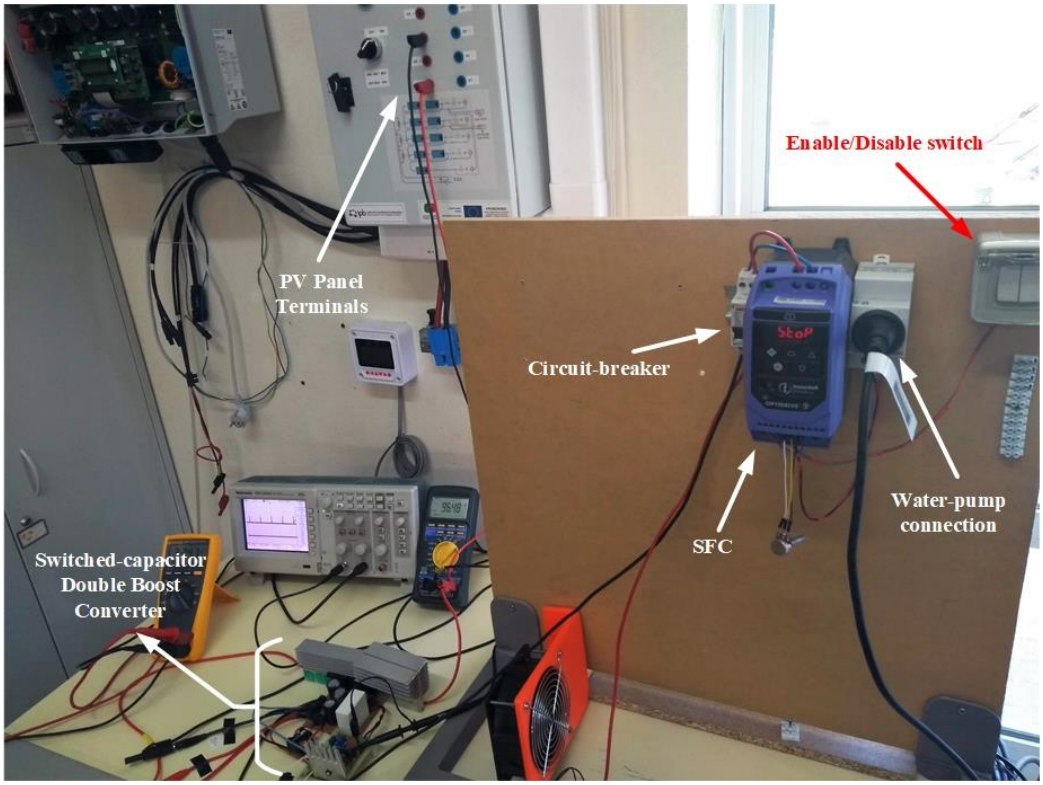


**Figure 34:** Experimental platform - Low power PVWPS test setup

(a) (b)

**Figure 35:** PV modules employed on tests - (a) REC275PE and (b) Fluitecnik FTS-220P

The water pump used for the tests was the Sterwins 750 DW-3 (**Figure 36**). The water pumps suggested in the Section 3.1 (**Table 2**) were not employed because the Sterwins was the one available in the laboratory.

The water tank utilized has storage capacity of 1000 liters (**Figure 36**). The hydraulic circuit was improvised using a long pipe with an elevation of approximately 2mH2O, in order to request power from the water pump. Before starting the tests with the

PVWPS, the Sterwins water pump was connected to the SFC and powered with the local electrical grid. This was made to verify the amount of power that the employed hydraulic circuit was requesting from the pump. The maximum value accused by the Invertek drive was approximately 300W at its output.

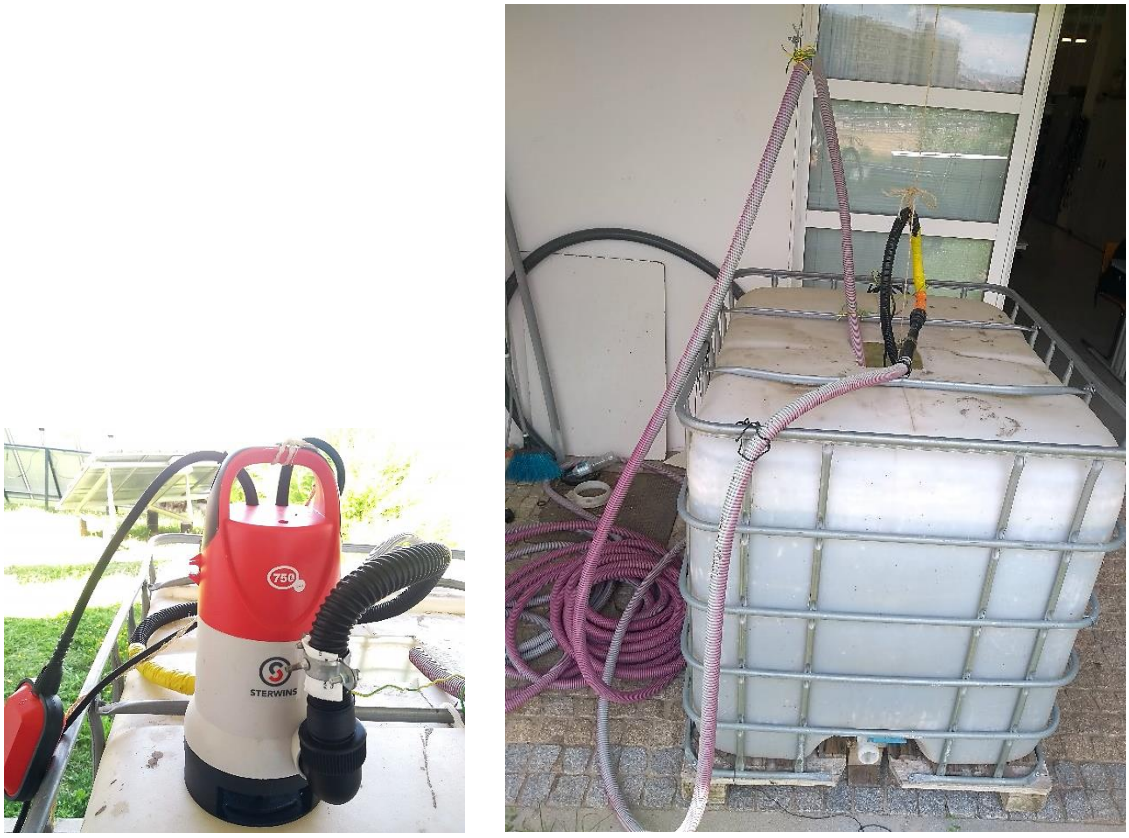


(a) (b)

**Figure 36:** (a) Water-pump and (b) Hydraulic circuit employed on tests.

As it was presented, the tests were performed under distinct weather conditions and distinct PI controller parameters. Different values of Kp (proportional gain) and Ki (integral time) were employed in order to verify which combination would result in a better operation of system, considering environmental variations such as daily solar irradiance and partial shadings. The two distinct configurations of the test's setup are presented in the following **Table 9**.

**Table 9:** Tests setup used on the PVWPS tests.

| Equipment | Description | Test Setup | | Figure |
|---|---|---|---|---|
| | | 1 | 2 | |
| PV modules | 3 x REC275PE | X | | Figure 35 (a) |
| PV modules | 3 x FTS220P | | X | Figure 35 (b) |
| Step-up Converter | SCDB converter | X | X | Figure 26 |
| SFC | Invertek Optidrive E3 | X | X | Figure 29 (b) |
| Water pump | Sterwins 750 DW-3 / 1-phase/ 750V / 230$V_{ac}$ / 7mH2$O_{max}$ | X | X | Figure 36 (a) |
| Water Tank / Hydraulic head | 1m³ / ≈2mH2O | X | X | Figure 36 (b) |

The **Table 10** shows the conditions of each test performed, according to the setups presented in the **Table 9**.

**Table 10:** Tests performed with the low power PVWPS solution.

| Test | Conditions | | | | | |
|---|---|---|---|---|---|---|
| | Setup | Day | Kp | Ki | Vi (PV)[1] | DC-link setpoint[2] |
| 1 | 2 | 22/05/2020 | 10 | 1 | ≈84V | 300V |
| 2 | 1 | 28/05/2020 | 1 | 4 | ≈94V | 310V |
| 3 | 1 | 28/05/2020 | 10 | 10 | ≈93V | 295V |
| 4 | 2 | 29/05/2020 | 1 | 10 | ≈92V | 320V |
| 5 | 2 | 29/05/2020 | 1 | 20 | ≈88V | 295V |
| 6 | 1 | 29/05/2020 | 8 | 3 | ≈94V | 295V |
| 7 | 2 | 01/06/2020 | 8 | 3 | ≈85V | 300V |
| 8 | 2 | 05/06/2020 | 2 | 8 | ≈83V | 300V |

[1]Input voltage of the SCDB converter, adjusted by a potentiometer in the control circuit of the converter (at the 1IN+ pin of the TL494) according to the voltage provided by the PV panel.
[2]PI reference for the DC-Link voltage, set by the potentiometer connected to the terminals 5,6 and 7 of the SFC.

It must be noticed that the voltage provided by the PV string (Vi) is configured at the beginning of each test. Its value determinates the power provided by the PV string (as it was explained in Section 4.1). Usually the MPP voltage value for a PV panel is 80% of its open-circuit voltage $V_{oc}$.

# 5. Results and Discussion

The values of the DC-link voltage, as well as the frequency and power of the motor-pump were acquired every 5 minutes at each one of the performed tests (previous **Table 10**). The solar irradiance levels during the time of the tests were obtained by the sensor of ESTiG PV system. The sensor is directed south and positioned at a 35° inclination, in the rooftop of the building (IPB - Bragança, Portugal).

The following **Figures 38 - 46** present the graphs elaborated with the acquired data. Each graph shows a linear interpolation for the solar irradiance, the DC bus voltage, the water pump frequency and power in relation to the hour of the day. The minimum and maximum values for the DC-link voltage and the AC power during the period of the test are indicated. The intent of the graphs is to illustrate the response of the water pumping system in relation to the solar irradiance variation, so it can be analyzed with which combination of Kp and Ki parameters the system works at its best.

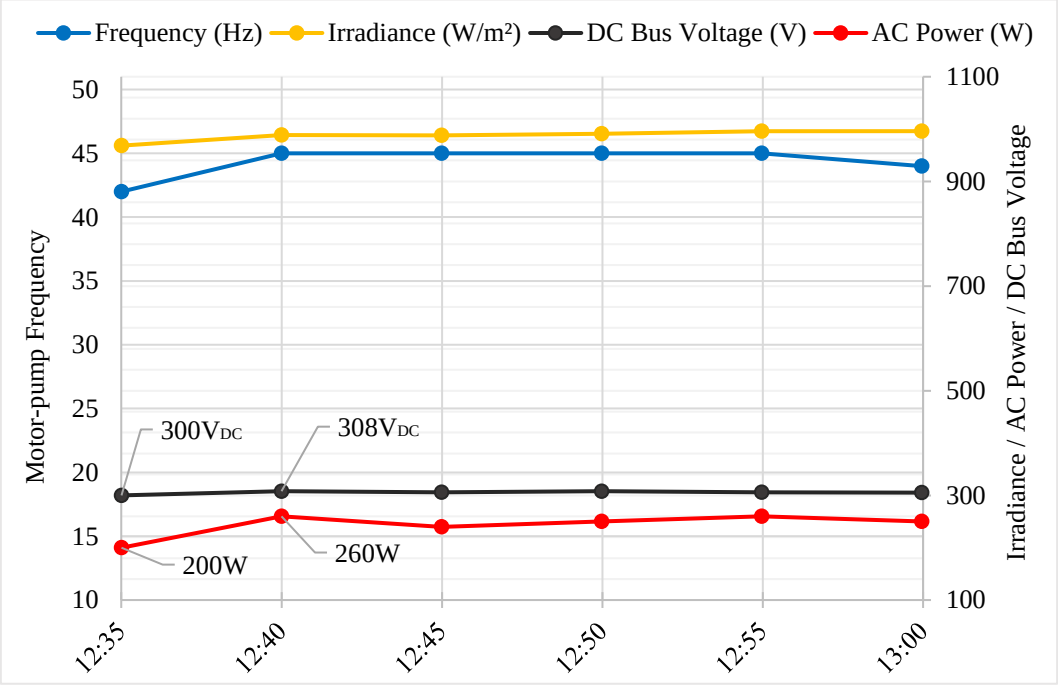


**Figure 37:** Results of the Test 1 performed with the low power PVWPS – Day 22/05/2020 at Bragança, Portugal.

**Figure 37** shows the results for the Test 1. This test was performed during the mid-day under great solar irradiance conditions (around 980W/m²) and with minimal variations. The proportional gain and integral time parameters were, respectively, 10 and

1. It can be seen that the DC-link voltage varied from 300V to 308V in the initial starting period and then stabilized around 305V. The setpoint was configured at 300V.

During the period of the Test 1 the water pump did not reach a power level around 290-300W, which was the maximum value that the hydraulic system setup could require for the pump (as mentioned in the previous Section 4.3).

The maximum power that the PV string of the Fluitecnik modules (Test Setup 2) could provide was 660W (220W x 3), but this considering an irradiance of 1000W/m²; cell temperature of 25°C; and operating at the MPP voltage. For the test conditions, the power provided by the PV string was probably not enough to supply 300W for the pump plus the losses of the SFC and the SCDB converter.

It must be highlighted that, according to an information provided by the LSE technician, one of the Fluitecnik modules of Setup 2 may present a damaged cell. This situation impacts the power provided by that module.

It can be seen that during the Test 1 the AC power presented a high oscillation going from 200W to 260W and back to 240W during the first 10 minutes. A longer period of test time would be needed for a more conclusive result regarding the response of the system to the PI parameters Kp=10 and Ki=1.

The following **Figure 38** shows the result for the Test 2. This test was performed from 15h to 16h under unstable weather conditions (solar irradiance varying in 528W/m²). The PI parameters Kp was 1 and Ki was 4. The setpoint for the DC-link was 310V.

It must be emphasized that the irradiance on the PV string of the REC modules (Test Setup 1) does not present the same values acquired by the sensor positioned on ESTiG rooftop. The REC modules were positioned outside the LSE directed southwest. Thus, the irradiance showed on the graphs of the tests performed with Setup 1 are only for a reference regarding the weather situation of the day.

During the first half hour of the Test 2 it can be seen that the frequency increased in 3Hz in response to the irradiance changes. This response maintained the DC-link voltage around 319V. At 15h30 a cloud shading occurred, changing drastically the power provided by the PV panel. As a result, the frequency of the water pump decreased to 28Hz, so in this period of time it was not able to maintain the DC bus voltage around the setpoint. It can be noticed that even with cloud shadings the motor-pump did not stopped pumping water.

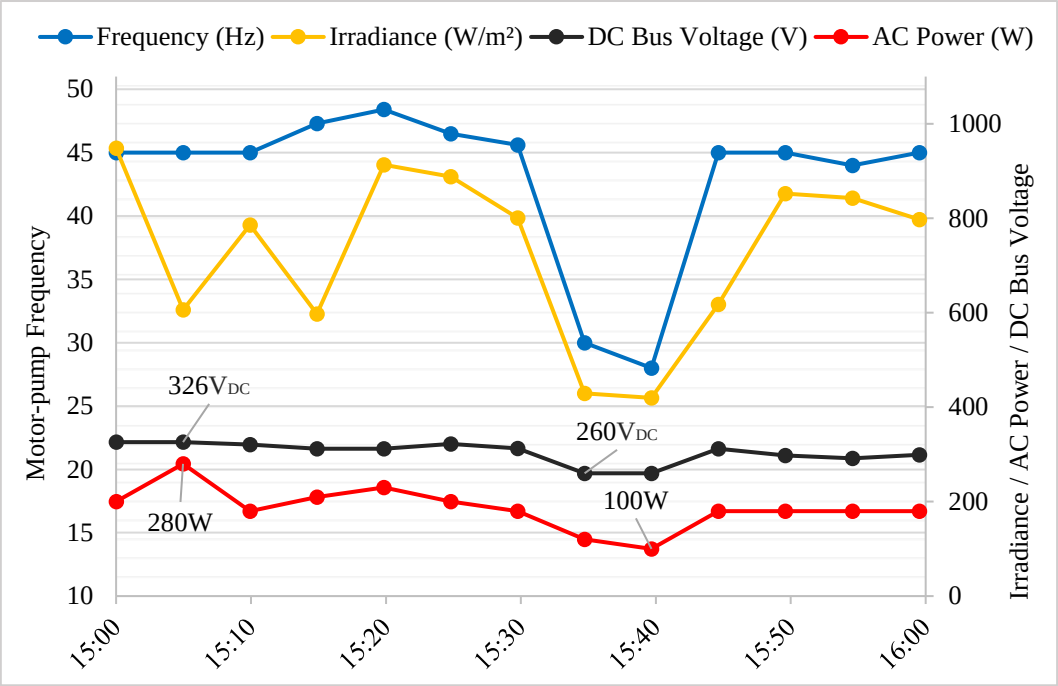


**Figure 38:** Results of the Test 2 performed with the low power PVWPS – Day 28/05/2020 at Bragança, Portugal.

The system returned to a stable operation after the cloud shading. But power levels around 290-300W were not achieve. The input voltage configured in the SCDB's potentiometer, the one responsible for selecting an optimum PV voltage level, was set around 92-96V. The MPP voltage of the panel with the REC modules is 94,5V, but this value is for the STC (Irradiance=1000W/m² and Cell temperature=25°C). For the conditions of the test, the MPP voltage would be lower, so, a better tuning of the potentiometer would provide more power to the pumping system. Also, the low values combination of the proportional gain and the integral time could have affected the power x frequency response of the system.

The **Figure 39** shows the result for the Test 3. This test was performed in the same day of the Test 2, but with PI parameters of Kp=10 and Ki=10 and a DC-link setpoint of 295V. It can be seen that the reduction of the setpoint and the high increment on the proportional gain made possible for the water pump to achieve 50Hz. The frequency response was able to maintain the DC-link voltage level around 300V even with the drastically decrease on the irradiance. But a power around 290-300W was not achieved, this was due to a combination of the low irradiance levels (considering that was late afternoon) and adjust of the PV array voltage.

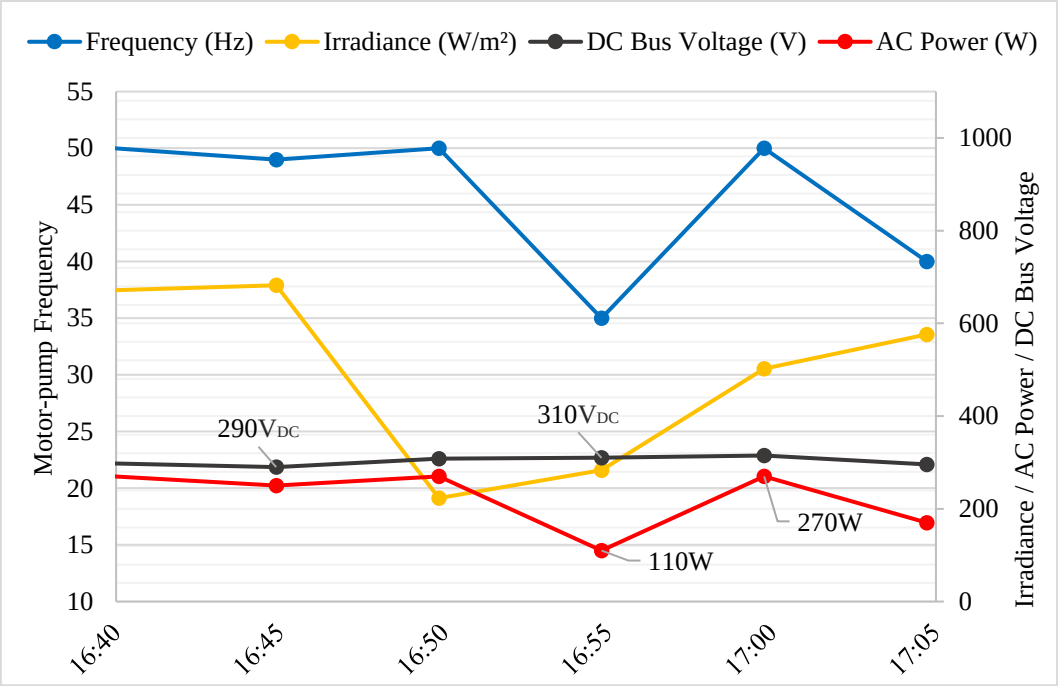


**Figure 39:** Results of the Test 3 performed with the low power PVWPS – Day 28/05/2020 at Bragança, Portugal.

**Figure 40** presents the results of Tests 4 and 5, which were made in sequence (without turning-off the PVWPS). The Test 4 was performed with Kp=1 and Ki=10, also, the DC-link setpoint was 320V and the PV panel voltage was at 92V. It can be seen that until 12h15 the system presented a slow and steady response according to the irradiance increase, maintaining the DC bus voltage around 325V. But the power of the water pump was low, meaning that a better tune of the PV panel voltage should have been made.

At 12h15 some parameters were changed (Test 5). The Ki was increased to 20, the DC-link setpoint was decreased to 295V and the PV panel voltage was set at 88V (closer to the MPP voltage of the panel). It can be seen that the frequency and power of the water pump increased, maintaining the DC bus voltage around 296V (close to the setpoint).

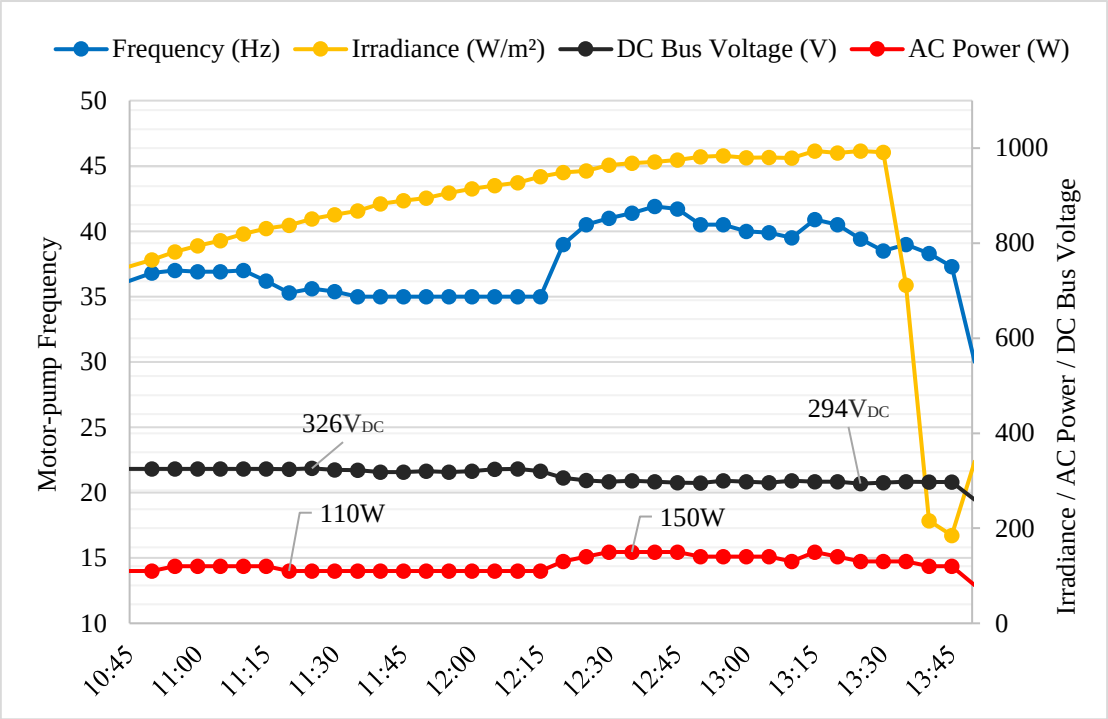


**Figure 40:** Results of the Tests 4 and 5 performed with the low power PVWPS – Day 29/05/2020 at Bragança, Portugal.

The system stopped working when clouds appeared, as the PV panel could not provide enough power. The **Figure 41** below shows the weather situation at which the system stopped running.

**Figure 41:** Weather condition at 13:45 of 29/05/2020 in Bragança, Portugal.

The Test 6 was performed later in the same day that of the Tests 4 and 5, but with the Setup 1. The results are shown in the **Figure 42**.

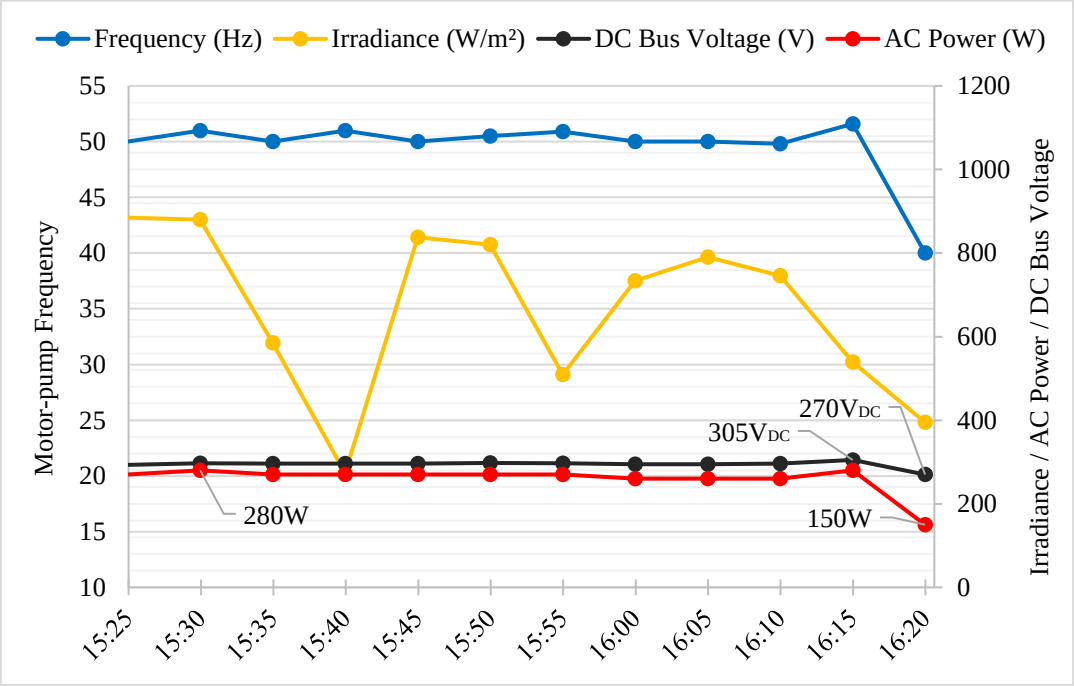


**Figure 42:** Results of the Test 6 performed with the low power PVWPS – Day 29/05/2020 at Bragança, Portugal.

In the Test 6 the parameter used for Kp and Ki were, respectively, 8 and 3. The DC-link setpoint was maintained in 295V. It can be seen that during this test the water pump worked at its best in comparison to the previous tests. The PI controller parameters manage to maintain the system stable with low amplitude oscillations. The power was stabilized around 280W, but the frequency was constantly oscillating around 50,5Hz until the moment that the irradiance fell drastically due to a possible cloud shading and the system stopped running.

The irradiance shown on the results for the Test 6 (**Figure 42**) may not reflect the actual irradiance on the PV panel (Setup 1). This is because the sensor is located in the roof of ESTiG, approximately 40m from the place where the Setup 2 was located.

The Tests 7 and 8 were performed in order to verify with more precision with which parameters the PVWPS would work better considering a whole day operation. The results of Test 7 are presented in the **Figure 43**.

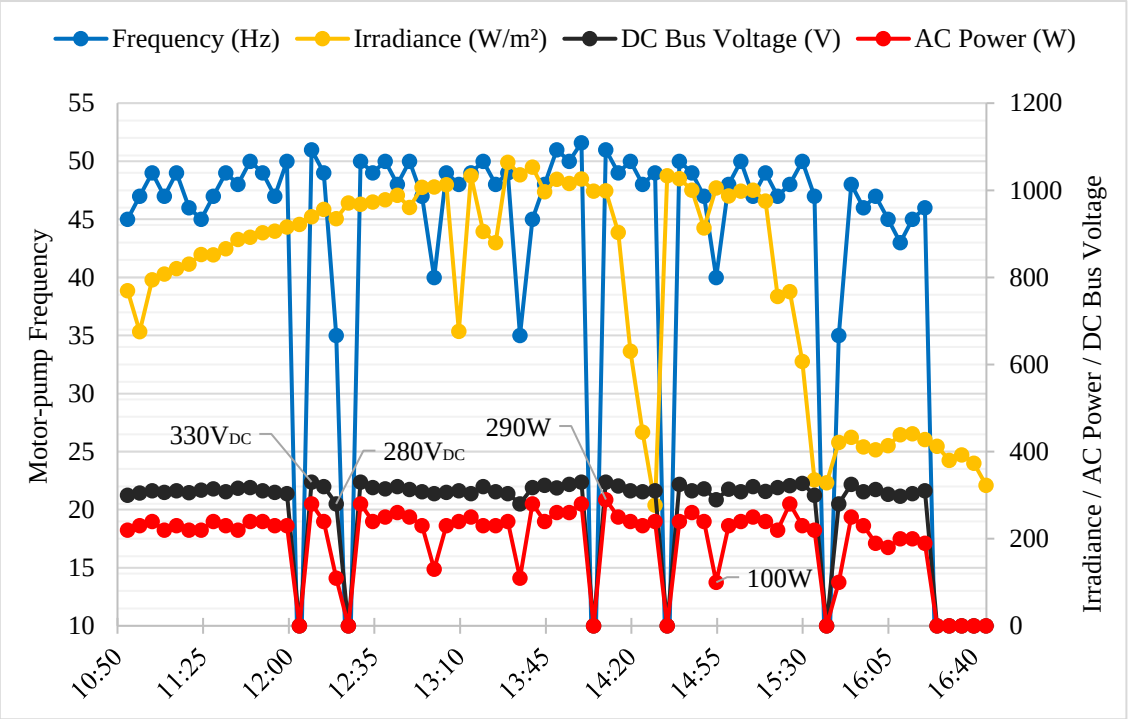


**Figure 43:** Results of the Test 7 performed with the low power PVWPS – Day 01/06/2020 at Bragança, Portugal.

The Kp and Ki parameters used in the Test 7 were the same as the Test 6, Kp=8 and Ki=3. The setpoint of the DC bus voltage was put at 300V and the PV panel voltage was adjusted to be closer to the MPP value, approximately 85V.

The test duration was from 10h50 to 16h40, until the irradiance levels (around 380W/m²) were not sufficient for the system to continue running. As showed in the **Figure 43**, the behavior of the system was very oscillatory and with fast shutdowns in moments of cloud shadings. The **Figure 44** shows the weather condition (cloudy sky) of the day 01/06/2020 at 14h10. The SFC accused under-voltage 5 times during the test, so the system had to be manually turned-off and then turned-on (some seconds later).

**Figure 44:** Weather conditions at 14:10 of 01/06/2020 in Bragança, Portugal.

The oscillatory behavior of the system during the Test 7 is a result of the PI controller parametrization. The low value of the integral time provided a quick and highly oscillatory response, that, combined with the higher value of Kp, made the system unstable according to the irradiance changes.

For Test 8 the PI parameters were corrected and a better functioning of the system was achieved. The parameter Kp was decreased to 2 and Ki was increased to 8. The **Figure 45** shows results of the Test 8.

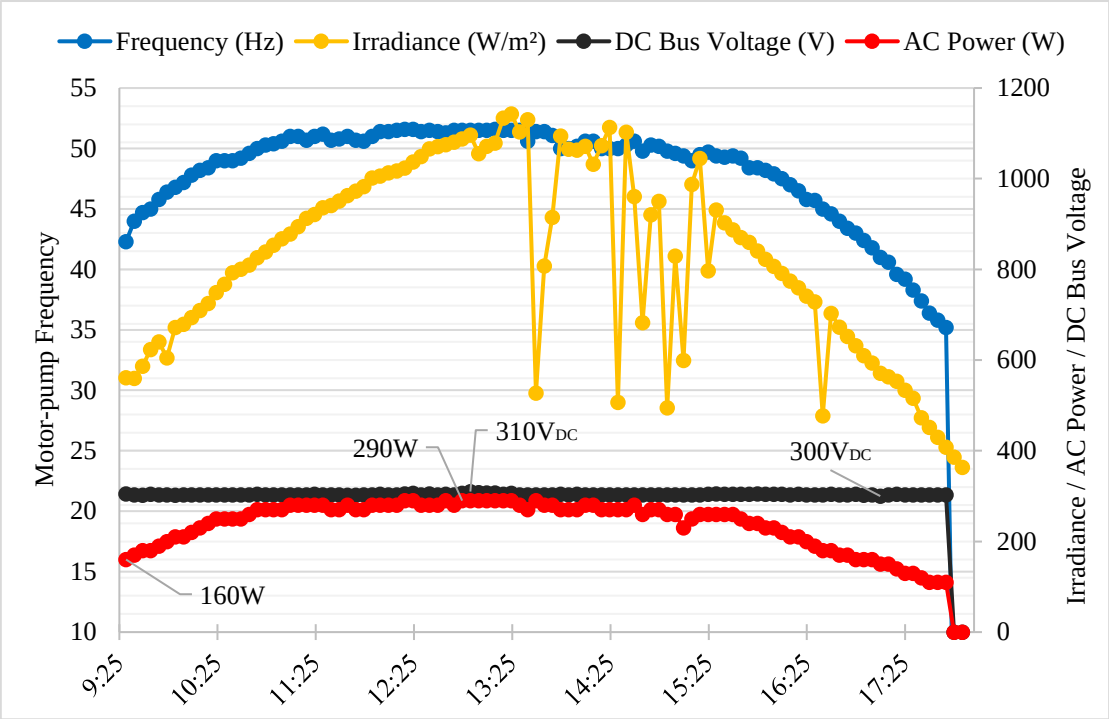


**Figure 45:** Results of the Test 8 performed with the low power PVWPS – Day 05/06/2020 at Bragança, Portugal.

As can be seen, the system was turned on at 9:25 (manually) and continued to work uninterruptedly until 17:55, when the irradiance levels fell below 400W/m³. The DC-link setpoint was 300V (such as the Test 7) and the PV panel voltage was also configured approximately to the MPP point (83V).

The DC bus voltage was maintained at 303V during most of the test period. In the moments of cloud shading, the PI controller worked well by slightly decreasing the frequency of the pump in order to control the DC bus voltage. It can be seen that the power of the water pump responded to the irradiance changes during the day. During the mid-day, the water pump worked around 290W, which was the maximum power that the experimental hydraulic circuit required for the pump.

By analyzing all the tests' results it can be concluded that the PVWPS proposed operates with more stability and reliability with lower Kp values (1 or 2) and higher Ki values (8 or 10). Also, can be perceived that the PV panel must be configured as close as possible to the MPP voltage, in the case of the tests it was around 82-84V. A DC-Link set point from 295V to 310V provided a better PVWPS functioning.

The tests performed with the experimental platform validated the proposed solution for a PVWPS. The results prove that, with the correct configuration, the system operates satisfactorily from morning until late afternoon, responding well to irradiance

changes due to weather conditions. For a future work, in order to verify the functioning of the system at its nominal power (750W), tests with another hydraulic system shall be performed.

Regarding the Switched-Capacitor Double Boost converter, its operation was validated and the first lab-model worked as expected. The **Figure 46** shows the measurement of the MOSFET command (gate-source). It was verified that the switch worked at a frequency value around 100kHz, which was the calculated value. The voltage peaks seen in the turning-on of the switch may be the result of the circuit layout. To solve this, in the second version of the lab-model, must be foreseen a better distribution of the components and shortened the length of the current paths around the switch-node.

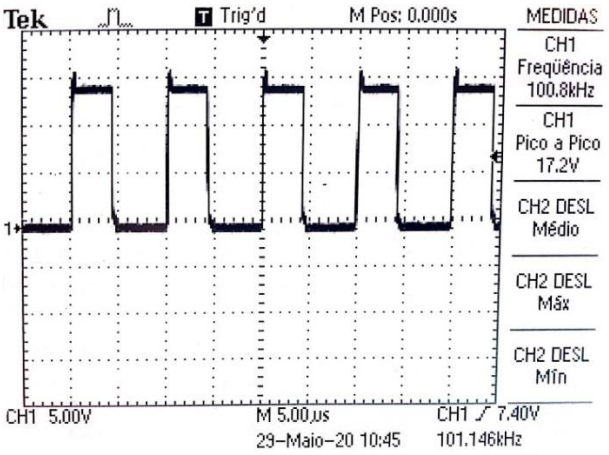


**Figure 46:** Oscilloscope screen of the switch command - MOSFET gate.

It was verified that the limitation of the SCDB converter output voltage worked. When the motor pump was turned off, the output voltage was maintained at 340V, which was the value adjusted by the potentiometer. The protection of the SFC in no load situations was ensured.

The output of the proposed converter presents two capacitors, C1 and C2 (as seen in the **Figure 25**). If the switched-capacitor stage works properly, the voltage across each capacitor must be approximately equal (half of the total output voltage of the converter), as it was exposed in Section 3.2.1.

The **Figures 48** and **49** show the PV voltage; the total output voltage of the SCDB converter; and the voltage across C1 for two situations. The first figure is for when the proposed PVWPS is running the water pump and the second is for when the water pump is off.

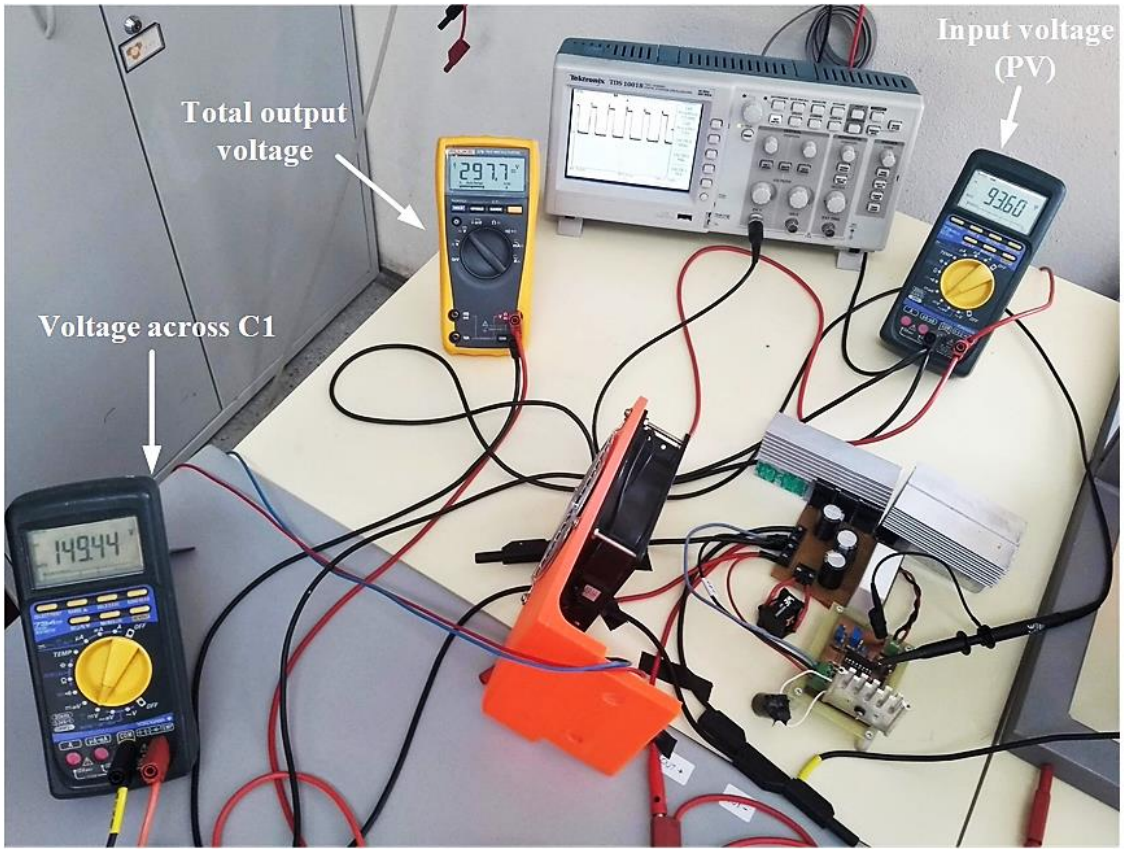


**Figure 47:** Voltage measurements when the PVWPS is running the water pump.

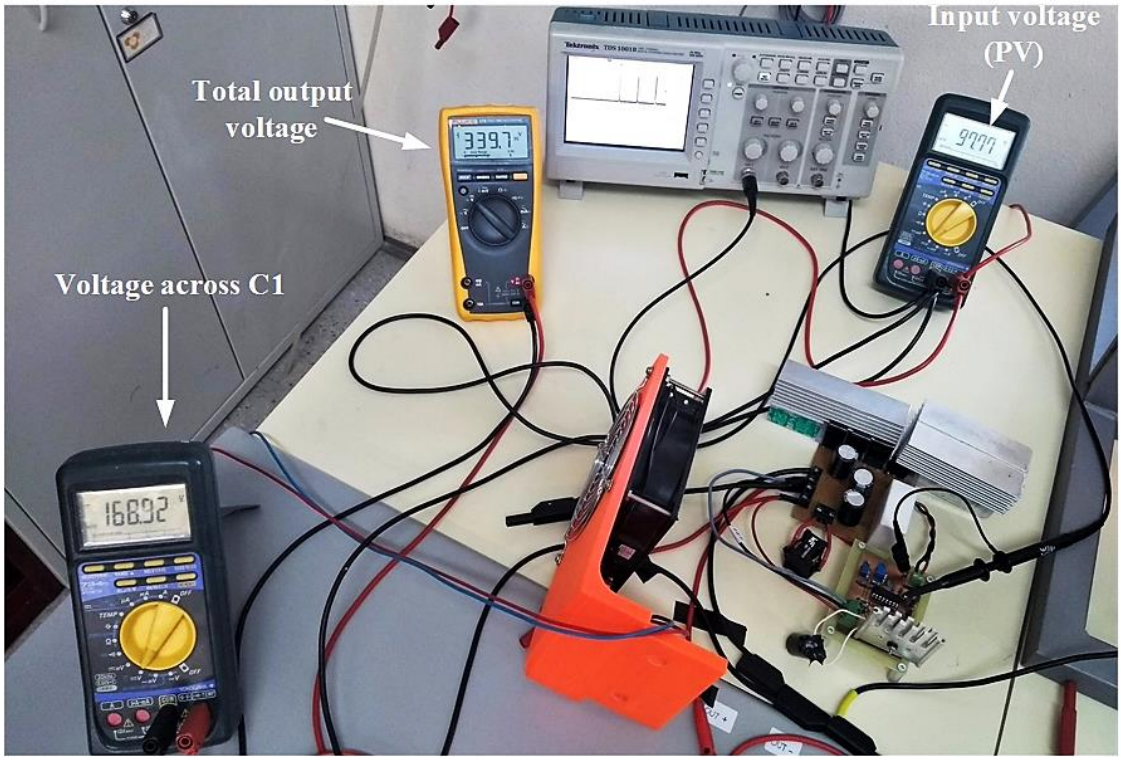


**Figure 48:** Voltage measurements when the PVWPS has no load.

It can be seen by the **Figure 47** that, at a given time at which the water pump is running, the output voltage of the DC-DC converter is at 297.7V and the voltage across capacitor C1 is at 149.44V. This shows that the voltage values across the output capacitors are approximately half of the total output voltage.

By analyzing the **Figure 48** it can be noted that, when the water pump is not running, the output voltage was limited at 339.7V. The configured value in order to protect the SFC was 340V. It can also be seen that the voltage across capacitor C1 is 168.92V, continuing to be approximately half of the total output voltage of the converter.

The results showed that the switched-capacitor stage of the SCDB converter worked as expected. Also, it can be verified that the control function regarding the output voltage limitation was effective.

One of the issues encountered during the tests was the heating of some components. The inductor and the MOSFET were the power-stage components that presented the major heating. Also, the voltage regulator TL783 showed high working temperatures. The solution was to add heat sinks at the MOSFET, diodes, voltage regulator, as well as use fan coolers. In this case the heat was controlled and the operation of the components was not compromised.

Regarding future improvements of the suggested PVWPS, it must be considered the addition of another control at the SFC (or use a different SFC). This another control would be responsible for turning-off the pumping system in cases of under voltage, in cloud shading moments, for example. Also, it is necessary to automatically start/stop the pumping system in the early morning and the late afternoon when the irradiance levels are not enough to provide the required power. The standby function of the Invertek drive does not suit the desired control function. The standby is only triggered after a short period of time (maximum 60s) of the motor-pump running at the lowest configured frequency, and this situation in a water pumping system does not require a shut down. Sometimes during the day, the water pump will run at its lowest frequency.

A second lab-model of the SCDB converter is on its way, some changes will be made, regarding the PCB layouts and some components. A preliminary mechanical design must be made in order to take one more step on turning the SCDB converter into a product.

### 5.1.1. Challenges and Difficulties

The major challenge faced by this work involves all of the questions regarding a real product development, considering an industry/company perspective. The time, resources, priorities and requirements when developing a solution for an industry are extremely different than doing it only for academic purposes. Students are not used to think and act in a “market/industry way” when executing their work.

Regarding the technical challenges encountered along the way, it can be mentioned the use of standard frequency converters in PVWPS. Operating and configuring an SFC in order to correctly work in a PVWPS require a careful analysis and understanding. Each SFC works in a different way and may present distinct functions. So, to ensure that the suggested layouts of PVWPS will work, an independent analysis and tests must be made for each system composition.

The pandemic situation due to the COVID-19 affected the course of this work. The access to the laboratory during the final part of the work was hindered. The time available for tests and improvements were reduced.

# 6. Conclusions and Future Work

This work presented innovative solutions for low power PVWPS. The initial goal was to develop a low power cost effective PVWPS, which suits the requirements presented by VALLED; is not oversized in terms of DC power; is modular; and employ only conventional components (from a company perspective).

The main goal was achieved. A complete solution for a low power PVWPS was developed and validated. It was tested a 750W PVWPS employing 3 PV modules; the SCDB converter; an SFC; and a single-phase 1HP water pump. Additionally, four low power PVWPS solutions were designed and suggested to VALLED. It was presented the equipment that could be employed at each solution.

For composing the proposed systems, it was developed a DC-DC voltage step-up converter, which was employed to solve the oversizing problem of the PV panel on low power PVWPS.

The tests' results were satisfactory. The PVWPS was tested in different weather conditions and the operation was in accordance of what was expected. Even employing the first lab-model of the SCDB converter on tests, the solution showed promising results.

The operation of the SCDB converter showed that its applicability can be wider than only for PVWPS, making possible for application in other types of PV systems.

A second lab-model of the SCDB it is on its way. Some improvements are being made, according to the issues encountered throughout the tests. The next step is to finish the assembling of the second prototype and test a PWWPS in an environment more similar to the field one.

The challenge from now on for making the SCDB converter to become a product involves the extensive cycle of improvements and real conditions testing. This must be done in cooperation with VALLED, in order to obtain a reliable, robust and cost-effective product.

For future works it is proposed to test the other low power PVWPS solutions and with the other suggested SFCs, PV modules and water pumps.

It is also recommended to be made an economical evaluation of the SCDB converter. This would make it possible to verify if the employment of the proposed voltage step-up converter would be cheaper than over-sizing the PV panel.

# References


[1] Vtas, P., & Pal, Y. (2017, August). **Solar PV array buck-boost converter fed single phase induction motor drives for water pumping.** In 2017 International Conference on Information, Communication, Instrumentation and Control (ICICIC) (pp. 1-5). IEEE.

[2] Slaymaker, Tom & Bain, Robert. (2017, March). **Access to drinking water around the world – in five infographics**. Published at The Guardian. Access: https://www.theguardian.com/global-development-professionals-network/2017/mar/17/access-to-drinking-water-world-six-infographics

[3] Araya, M. K. (2010). **Photovoltaics for Community Service Facilities Guidance for Sustainability**. Africa Renewable Energy Access Program (AFREA).

[4] Ministry of Energy and Waters. (2018, January). **Program "Água para Todos"**. Access:.https://www.minea.gov.ao/index.php/projectos/category/134-painel-iii?download=433:pat

[5] Angolan State Secretary for Water interview (2020, March). Access: http://jornaldeangola.sapo.ao/entrevista/precisamos-de-triplicar-ou-quadriplicar-os-investimentos-em-abastecimento-de-agua

[6] Oliveira de Melo, R. (2004). **Condicionamento de potência de uma motobomba em um sistema de bombeamento fotovoltaico através de um conversor de frequência.** Master's dissertation, Federal University of Pernambuco.

[7] Scortegagna, A. K. (2019). **Photovoltaic water pumping systems based on standard frequency converters.** Master's dissertation, Polytechnic Institute of Bragança.

[8] A. K. Scortegagna, V. Leite and D. Roman. **New Approaches for Low Power Photovoltaic Water Pumping Systems**. IECON 2019 - 45th Annual Conference of the IEEE Industrial Electronics Society, Lisbon, Portugal, 2019, pp. 2428-2433.

[9] Roman, D. J. V. (2018). **Photovoltaic water pumping systems based on standard components**. Master's dissertation, Polytechnic Institute of Bragança.

[10] Alonso Abella, M., Lorenzo, E., & Chenlo, F. (2003). **PV water pumping systems based on standard frequency converters.** Progress in Photovoltaics: Research and Applications, 11(3), 179-191.

[11] T.A Binshad, K. Vijayakumar and M. Kaleeswari, **PV based water pumping system for agricultural irrigation.** (2016, September). Volume 10, Issue 3, pp 319-328.

[12] Eker, B. (2005). **Solar powered water pumping systems**. Trakia Journal of Sciences, 3(7), 7-11.

[13] Furtado, A. M. S. (2016). **Técnicas de seguimento do ponto de máxima potência para sistemas fotovoltaicos com sombreamento parcial.** Master's thesis, Universidade Federal de Pernambuco.

[14] dos Santos, W. S. (2016). **Sistema fotovoltaico de bombeamento baseado em conversores de frequência e bombas centrífugas comerciais utilizando controle fuzzy externo com tensão fixa.** Doctoral dissertation, Federal University of Pará.

[15] Yaskawa J1000 technical manual. Access: https://www.yaskawa.com/products/drives/industrial-ac-drives/microdrives/j1000-drive/-/content/_6a26e78e-b18f-4523-a933-6d7989ed5f0e_CoreManuals

[16] Narayana, V., Mishra, A. K., & Singh, B. (2017). **Development of low-cost PV array-fed SRM drive-based water pumping system utilizing CSC converter.** IET Power Electronics, 10(2), 156-168

[17] Caracas, J. V. M., de Carvalho Farias, G., Teixeira, L. F. M., & de Souza Ribeiro, L. A. (2013). **Implementation of a high-efficiency, high-lifetime, and low-cost converter for an autonomous photovoltaic water pumping system.** IEEE Transactions on Industry Applications, 50(1), 631-641.

[18] Gügner, M., & Özbayer, M. M. **Centrifugal Pump Design Materials and Specifications.** Eskisehir Technical University of Science and Technology. Journal B-Theoretical Sciences, 8(1), 143-153.

[19] Chandel, S. S., Naik, M. N., & Chandel, R. (2015). **Review of solar photovoltaic water pumping system technology for irrigation and community drinking water supplies**. Renewable and Sustainable Energy Reviews, 49, 1084-1099.

[20] LORENTZ Helical Rotor Pumps. Access: https://www.lorentz.de/products-and-technology/technology/helical-rotor-pumps

[21] LORENTZ Submersible Solar Pumps. Access: https://www.lorentz.de/products-and-technology/pump-types/submersible-solar-pumps

[22] Ideal Delta Submersible Water Pump. Access: https://idealdelta.com/submersiveis/

[23] Li, G., Jin, Y., Akram, M. W., & Chen, X. (2017). **Research and current status of the solar photovoltaic water pumping system – A review**. Renewable and Sustainable Energy Reviews, 79, 440-458.

[24] Tomar, A., & Mishra, S. (2016, July). **Multi-input single-output DC-DC converter based PV water pumping system**. In 2016 IEEE 1st International Conference on Power Electronics, Intelligent Control and Energy Systems (ICPEICES) (pp. 1-5). IEEE.

[25] Miladi, M., Bennani-Benabdelghani, A., & Belkhodja, I. S. (2018). **An Efficient and Low-Cost Single-Stage PV Pumping System: Experimental Investigation Based on Standard Frequency Converter**. International Journal of Renewable Energy Research (IJRER), 8(1), 108-119.

[26] Saini, A. K., & Dubey, A. K. (2017). **Performance Analysis of Single Phase Induction Motor with Solar PV Array for water Pumping System**. Intl. J. Eng. Res. Technol, 6, 721-727.

[27] Jana, B., Dhandhukiya, S., Tiwari, R., & Babu, N. R. (2019). **A Study of DC–DC Converters with MPPT for Standalone Solar Water-Pumping System**. In Recent Developments in Machine Learning and Data Analytics (pp. 373-381). Springer, Singapore.

[28] Sharma, U., Kumar, S., & Singh, B. (2016, July). **Solar array fed water pumping system using induction motor drive.** In 2016 IEEE 1st international conference on power electronics, intelligent control and energy systems (ICPEICES) (pp. 1-6). IEEE.

[29] Dalberg & Efficiency for Access Coalition Secretariat. (2019). **Solar Water Pump Outlook 2019: Global Trends and Market Opportunities.** Access: https://efficiencyforaccess.org/publications/solar-water-pump-outlook-2019-global-trends-and-market-opportunities

[30] Grundfos Solar Water Solutions. **Solar-Powered Water Supply - Unmatched Flexibility for Water Services to Communities.** Access: https://www.grundfos.com/market-areas/water/solar-water-solutions.html

[31] Forouzesh, M., Siwakoti, Y. P., Gorji, S. A., Blaabjerg, F., & Lehman, B. (2017). **Step-up DC–DC converters: a comprehensive review of voltage-boosting techniques, topologies, and applications**. IEEE Transactions on Power Electronics, 32(12), 9143-9178.

[32] Fey, A. N., Romaneli, E. F. R., Fernandes, L. G., & Gules, R. (2018, November). **A Switched-Capacitor Double Boost Converter for a Photovoltaic Application.** In 2018 13th IEEE International Conference on Industry Applications (INDUSCON) (pp. 126-130). IEEE.

[33] Morris, G. Q. (1996). **Magnetically integrated full wave DC to DC converter.** U.S. Patent No. 5,555,494. Washington, DC: U.S. Patent and Trademark Office.

[34] Pires, V. P. (2014). **Sintonia de um Controlador PID em um Sistema de Controle de Vazão.** Revista da Graduação, 7(2).

[35] Texas Instruments. **TL783 High-voltage Adjustable Regulator Datasheet.** Access: https://www.ti.com/product/TL783

[36] Texas Instruments. **TL494 Pulse-Width-Modulation Control Circuits Datasheet.** Access: https://www.ti.com/product/TL494

[37] Invertek Drivers. **Optidrive E3 - ODE-3-120070-1012-01 - Technical Manual**. Access: https://www.invertekdrives.com/variable-frequency-drives/optidrive-e3-single-phase/model-data/